NTNU
Norwegian University of
Science and Technology

The effect of cPLA2 inhibition in basal-like breast cancer

Madina Akan

MSc in Biology
Submission date: June 2016
Supervisor: Berit Johansen, IBI
Co-supervisor: Siver Andreas Moestue, DMF

Norwegian University of Science and Technology
Department of Biology

Abstract

Introduction: Altered metabolism in cells is a hallmark of cancer and cytosolic phospholipase A2 (cPLA2) is a ubiquitous enzyme involved in inflammation. Recent studies has also suggested a possible involvement in various cancer forms, including basal-like breast cancer. The objective of this project was to evaluate the effects of cPLA2 inhibition by the novel drug AVX235 on proliferation and metabolism in basal-like breast cancer in vitro and in vivo with special focus on choline and glucose metabolism.

Methods: Histopathological samples from patient-derived triple-negative BLBC models from previous studies were analyzed with respect to proliferative markers. The cytotoxicity of AVX235 on several breast cancer cell lines was measured. ^{1}H and ^{13}C NMR spectroscopy with MDA-MB-231 cells was performed and resulting metabolite profiles were evaluated by PCA and personal analysis.

Results: IC50 of AVX235 was identified around 27 µM for tested cell lines. ^{1}H NMR analysis of cell extracts gave well resolved spectra. AVX235 treated samples showed highest levels in all metabolites. ^{13}C NMR analysis showed different metabolite profile spectra and mitotic cells counting did not show inhibition of proliferation in breast cancer cells; however, results are not solid due to the limited data.

Conclusion: In these results, we observed that 10 µM concentration AVX235 has no inhibitory effect on proliferation of MDA-MB-231 cells in response to cPLA2 inhibition, which is supported by metabolic activity from ^{1}H NMR spectra results too. Data was limited by few samples or technical errors. Thus, the effect of AVX235 on proliferation and the choline and glucose metabolism needs more research.

ACKNOWLEDGEMENTS

This master's thesis was conducted at the Norwegian University of Science and Technology (NTNU), at the Faculty of Natural Sciences and Technology, Department of Biology with collaboration of MR Cancer Group, Department of Circulation and Medical Imaging, NTNU, in the period between September 2014 and June 2016.

I would like to express my sincerest gratitude to my supervisors Professor Berit Johansen, Associate Professor Siver A. Moestue and Hanna Maja Tunset for providing me this opportunity. It has been privilege to learn from you. Thank you, Berit, for letting me be part of this interesting research, I gained great experience. Thank you, Siver, for your recommendations and for being very supportive. You taught me a lot about how to come to best scientific conclusions without explaining everything. I marvel at your patience with my slowness. Hanna Maja, I would like thank you for guidance and assistance during all my study period. Your advices and encouragements helped me a lot. In addition, I would like to thank Astrid Jullumstrø Feuerherm who always helped with useful lab hacks and bright smile. I thank everybody who assisted me and contributed in this study, all members of MR Cancer group and PLA2 lab. Everybody in there were so helpful and always available, I appreciate it all.

Finally, I am grateful for all support I received from my friends Meral, Erem and Julia for making my days in Trondheim memorable and fun.

Most importantly, I am thankful for my family, especially my parents who always believed in me and supported all my crazy ideas. Nurlan, thank you for just being there, it makes five folds difference.

Madina Akan

Trondheim, June 2016

List of abbreviation

AA: Arachidonic Acid

ad-PLA_2: Adipose phospholipase A_2

ATCC: American Type Culture Collection

AVX235: $cPLA_2$ -α inhibitor

BLBC: Basal like breast cancer

BRCA1/2: Breast cancer ½

Cho: Choline

CCC: Choline containing compounds

COX: Cyclooxygenase

$cPLA_2$-α: Cytosolic phospholipases A_2 –alpha

DMSO: Dimethyl sulfoxide

EGF: Epidermal growth factor

EGFR: Epidermal growth factor receptor

ER: Estrogen receptor

FBS: Fetal bovine serum

HER2: Human epithelial growth factor 2

IHC: Immunohistochemistry

LOX: Lipooxygenase

LPC: Lyso-phosphatidylcholine

LPLA2: Lysosomal phospholipase A2

MAPK: Mitogen activated phosphorylating kinases

MMP2: Matrix metalloproteinase 2

NMR: Nuclear Magnetic Resonance

NSAIDS: Non-steroidal anti-inflammatory drugs

PAF-AH: Platelet-activating factor acetyl-hydrolase

PBS: Phosphate buffered saline

PC: Phosphocholine

PtdCho: Phosphatidylcholine

PDT: Population doubling time

PGE_2: Prostaglandin E_2

PI: Phosphatidylinositol

PI3K: Phosphatidylinositol-3- kinase

PLA_2: Phospholipase A_2

PR: Progesterone receptor

RA: Rheumatoid arthritis

RPMI-1640: Roswell Park memorial institute -1640 medium

PPP: Pentose Phosphate Pathway

PTEN: Phosphatase and tensin analog

$sPLA_2$: Secretory phospholipase A_2

SD: Standard deviation

STAT: Signal transducer and activator of transcription

TCA: Tricarboxylic acid

TGFα: Transforming growth factor alpha

TNBC: Triple negative breast cancer

TNM: Tumour-node-metastases

VEGFR: Vascular endothelial growth factor receptor

List of content:

1. INTRODUCTION

1.1. Cancer

Cancer is an abnormal growth of cells with potential to spread and invade any other type of tissue in the body. There are more than 100 types of human cancer, reflecting that cancer can arise from most, if not all, tissues and cell types of body. Prognosis is different depending on the type. Cancer treatment can include pharmacotherapy and/or surgery [1].

According to the World Health Organization's (WHO) report in 2012, 14.1 million new cancer cases were diagnosed; 8.2 million people died from cancer; and 32.6 million people were five-year cancer survivors (people who are alive five years after being diagnosed with cancer). In the conclusion of this report, by 2025, 19.3 million new cancer cases are expected to be diagnosed each year [2].

After many years of rapid achievements, cancer research has generated an abundant and complex body of knowledge, concluding that cancer is a disease of genome changes. This has been proved by the discovery of mutations, which produce oncogenes getting dominant and tumor suppressor genes getting recessive function. Mutations or other changes in these two categories of genes are the major cause of healthy cells transforming into cancerous ones [3]. Both classes of cancer genes have been identified through their alteration in human and animal cancer cells. Their cancer phenotypes were detected in experimental models [4, 5]. These mutations may be caused by many factors such as: radiation, environmental factors, some chemicals or simply mistakes in DNA repair mechanisms of cells.

Cancer develops and progresses over time as mutations and genetic changes compile in cells. These traits, which a normal cell gains as it transforms into a precancerous one and in the end into cancer, are called the "Hallmarks of Cancer" [5]. The hallmarks of cancer give general idea how some chemicals may interact with cancer related genes and create carcinogenic combinations that can lead to carcinogenesis. To understand cancer development because of chemical exposure, it is helpful to understand the biology of cancer and how the disease progresses (Figure 1.1).

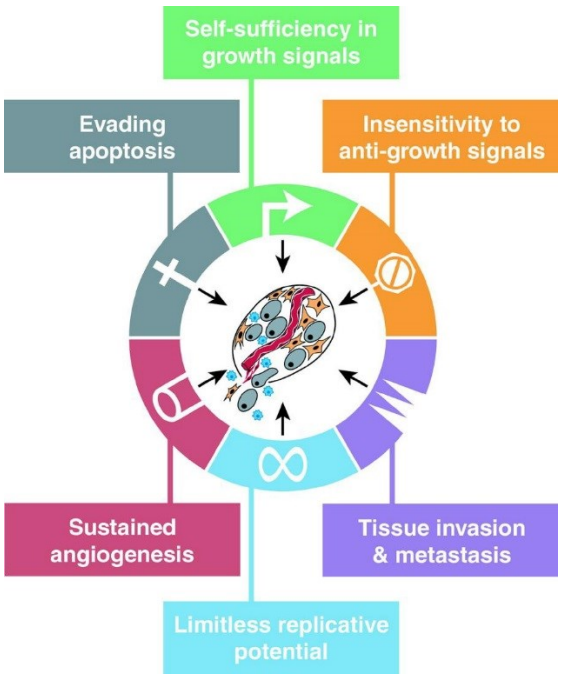

Figure 1.1: The classic hallmarks of cancer. Proposed general hallmarks of cancer of adapted mechanisms of surviving and development [4].

Normal healthy cells, excluding muscle cells, blood cells and nerve cells, replicate in order for the body to grow and maintain itself. Cancer develops when genetically changed cells begin to divide and proliferate uncontrollably. In contrast to normal cells, cancer cells do not respond to the external and internal signals that control cell division. Because cancer cells grow and divide without regulation, they quickly accumulate big masses, which may turn into tumor within tissue and organs. In the late stages of cancer, malignant tumors can metastasize and spread to another locations in the body. It breaks through tissue boundaries and form new tumors in other organs, which can lead to the shutdown of vital organ systems to lethal outcome [6, 7].

1.1.1. Breast cancer

Breast cancer is the leading cancer type in women worldwide. It leads to death accounting for 23% of (1.38 million) of the total new cancer cases and 14% (458 400) of the total cancer deaths in 2008. In Europe, 371 000 new cases of breast cancer diagnosed and 129 900 breast-cancer-related deaths were reported in 2004 [8]. About half the breast cancer cases and 60% of the deaths are estimated to occur in economically developing countries. In comparison, economically developed countries have been decreasing breast cancer death rates, mostly because of early detection through mammography and improved treatment [1, 9].

The classification of breast cancers is constantly evolving due to the advances in DNA and RNA microarrays as well as immunohistochemical (IHC) techniques. Breast cancer can be classified based on where in the breast the disease started (e.g., milk ducts, lobules), how the tumor grows, and other factors [10]. Breast tumor can be noninvasive (benign) or invasive (malignant); it is when cancer cells stay in one location invading surrounding tissues without spreading out, and when cancer cells migrate (metastasize) to another parts of body out of breast through bloodstream and lymph nodes, respectively [11]. Most malignant breast tumors are carcinomas, a type of cancer that starts in epithelial cells. There are ductal carcinoma in situ (DCIS) and lobular carcinoma in situ (LCIS), a noninvasive breast cancer types. In DCIS/LCIS cells abnormally lined in ducts and in lobules have changed their morphology to look like cancer cells. If these cells start to penetrate basal membrane to neighboring tissue and metastasize they become invasive breast cancer.

There are several risk factors which can lead to breast cancer development, like genes, aging, being overweight, and using hormone replacement therapy, taking birth control pills, or having dense breasts. There are two BReast-CAncer susceptibility genes: BRCA1 and BRCA2. They are tumor suppressor genes, which help to breast and ovarian cancer formation in their mutant phenotype forms [11, 12]. Normally large protein products of these two genes have several crucial roles in cell regulation, chromosomal stability, DNA repair and in response of cell to DNA damage [13].

Breast cancer is very diverse and complex in its subtypes; there are different methods to classify it. One is histopathological classification based on different biological features, like presence of hormone Estrogen Receptor (ER) and Progesterone Receptor (PR) and human epithelial growth factor 2 (HER2) status and clinical behavior.

Other classification is based on molecular foundation with consecutive patterns of genes [14]. The validity of both methods has been supported in several studies. Microarray expression profiling classifies breast cancer into five molecular subtypes: luminal A, luminal B, basal-like, HER2, and normal breast-like [15]. Luminal type of breast cancer has gene expression pattern similar to that of the estrogen receptor positive cells that are lined inside the duct and gland, its *lumen.* Luminal A breast cancer has better prognosis and slower growth rate, while luminal B breast cancer has worse prognosis and faster growth rate [16]. Recent research suggests a new subtype like claudin-low, characterized by low expression of luminal markers and high expression of mesenchymal markers [17, 18]. All these subtypes have different survival rates and prognoses.

Breast cancer molecular subtypes identified by these approaches have been suggested to have distinct clinical presentations, sites of relapse, histological features, responses to chemotherapy, and outcomes [19].

1.1.2. **Breast cancer treatment**

The choice of treatment in breast cancer is based on stage of the disease and the subtype of the tumor. Clinicians stage tumors by the Tumor size, the amount of spread to lymph Node and the range of Metastasis (TNM) international classification system [20]. A number is added to each letter that indicates the size and/or the extent of primary tumour and the degree of cancer spread. Results of these diagnostics affect the treatment plan. Since this is very personalized treatment, recommendations would depend on several factors like: the stage of the tumor, the tumor's subtype, including hormone receptor status (ER, PR) and HER2 status, genomic markers, the patient's age, general health, the patient's menopausal status, the presence of known mutations in inherited breast cancer genes, such as *BRCA1* or *BRCA2.*

Modern breast cancer treatment depends if it is localized disease or metastatic disease. Localized stage is when disease stays in breast; usually treatment involves surgical removal of tumor and it is always curative. Depending on grade of invasiveness, there are mastectomy removal of whole breast and lumpectomy (breast-conserving surgery) removal of only the tumor and tissues around it [21]. Patients often receive systemic treatment alongside surgery. Systemic treatment may be chemotherapy or hormone-targeted therapy, if cancer is receptor positive. Targeted therapy uses drugs such as lapatinib, pertuzumab, and trastuzumab against breast cancer cells that have high levels of a protein HER2 to prompt the body's immune system to destroy cancer [22]. Hormone therapy uses drugs like tamoxifen, anastrozole, exemestane, and letrozole to block certain hormonal activity against ER and PR from fueling the growth of breast cancer cells. Radiotherapy is usually used after surgery or whensurgery is not possible for patient. Radiation uses radiation waves to kill cancer cells and chemotherapies acts directly or indirectly on DNA or on the cell proliferation machinery. They affects both healthy and malignant cells and have many side effects, that is why they often accompanied with adjuvant (complementary) therapy [23]. Antracyclin containing chemotherapy is common example of adjuvant therapy after surgery to help cure cancer.

When chemotherapy is given before surgery then it is called neoadjuvant therapy. It is a step to try to shrink tumor before surgery to make the procedure less radical and conserve as much breast as possible. The treatment goal of metastases is to minimize symptoms and control invasiveness of diseases; it carries a palliative intent. One third of breast cancer patients would develop in distant metastasis and unfortunately will have lethal outcome. Nowadays there is no effective treatment against breast cancer distant metastasis, but there are variety of treatment options for improvement (pain relieve) and extension of life. In these cases usually combinations of all types of treatment are used to reduce cancer progression and try to enhance immune system at best [24].

In all cases, breast cancer treatment should start as early as possible. Therefore, health monitoring and early diagnostics play crucial role in cancer treatment in general.

1.1.3. **Basal-like breast cancer**

Almost 75% of basal like breast cancer (BLBC) is triple negative breast cancer (TNBC) due to the absence of estrogen or progesterone receptors and normal amounts of HER2 [25, 26]. BLBC usually has BRCA1 mutation and is very aggressive; tend to be of high grade characterized by exceptionally high mitotic indices, the presence of central necrotic or fibrotic zones, pushing borders, conspicuous lymphocytic infiltrate, and typical/atypical medullary features. Even after successful chemotherapy, it has high chance to reoccur in the first 5 years following therapy and patients tend to have low survival rate [27, 28].

BLBC constitutes 20% of all breast tumor cases, is more common in younger patients and African-American women, metastatizesearly, and more frequently relapses[29, 30]. Since they lack ER, PR, and HER2 expression patients having this disease have little benefit from targeted hormone therapy like trastuzumab and lapatinib and have chemotherapy such as doxorubicin and taxanes as their only option. A great deal of research is going on to find more effective ways to treat this disease [27]. There are different strategies in targeted therapies approved or still in preclinical trials, like inhibiting angiogenesis with bevacizumab in combination with other drugs, inhibiting EGFR with cetuximab either alone or with carboplatin, PARP inhibition with iniparib and olaparib and inhibition of Src kinases with dasatinib in combination with other medications [31].

Since BLBC is frequently associated with PIK3CA gene mutation, increased pAkt level and alteration of PI3K pathway, it makes sense to target it [32]. Activated PI3K promotes phosphatidylinositol triphosphate (PIP3) which activates Akt/protein kinase B (PKB) downstream. PKB downstream ends up in blocking inhibition of mammalian target of rapamycin (mTOR) and by promoting cyclin D1 [33]. This pathway regulateds initiation of cell proliferation, cell migration, and apoptosis inhibition. Several drugs, including BEZ235, have been developed to target PI3K/mTOR signaling. Such drugs can inhibit tumor growth in preclinical studies and are therefore being tested in clinical trials [32, 34].

1.2. Cancer cell metabolism

As it was stated in hallmarks of cancer, a malign tumor needs to proliferate, evade apoptosis, metastases, sustain angiogenesis, and be self-sufficient. All of it requires energy and building blocks, and cancer cell metabolism will be altered to accommodate these needs. Cancer metabolism is crucial and it is important to understand changed mechanisms [35, 36]. Metabolic traits of cancer are increased glycolysis, glutaminolysis, altered oxygen consumption, abnormal phospholipid metabolism, and increased dependency on reduced glucose metabolism [37]. To maintain high rate of proliferation cancer needs to change key metabolic pathways like tricarboxylic acid (TCA) cycle and pentose phosphate pathway (PPP). In addition, it needs control over genetic instabilities and gene expression to manipulate the connections between oncogenic signaling pathways and metabolic pathways [35, 38]. It also needs to maintain control over external signal responses.

All of these traits suggest that it may be a good target therapeutic strategy to cut the tumor's energy supply. Many new researches are started to develop drugs aiming weakness in cancer metabolic pathways [36].

1.2.1. Choline metabolism in cancer

Choline is essential nutrient, which we consume from various types of food. It has important role in cell integrity and signaling.

From previous studies, it was identified that breast cancer has altered metabolism in choline compared to normal breast epithelial cells, which are prone to proliferate in general. NMR

spectroscopy showed higher concentration of free choline (Cho), phosphocholine (PCho) and glycerophosphocholine (GPC); fingerprinting of altered cancer metabolism. Alongside with choline containing compounds (CCC) other choline transporters and proteins involved in choline metabolism pathway showed increased level on NMR spectra too [39, 40].

The role of altered choline metabolism in cancer is not fully understood. Choline is involved in phosphatidylcholine (Ptd-Cho) degradation, which is a phospholipid with choline head group and it takes part in cell membrane. It is increasing proliferation level in cells and recent studies show relation of this to cancer as it is associated to a constant changes in cell membrane due to growth [41]. Phospholipases cause phosphatidylcholine degradation and produce phosphocholine. Cytosolic phospholipase A2 (cPLA2) is catalyzing PtdCho degradation and producing GPC. Another pathway of phosphocholine and choline production is through catalytic activity of other members of phospholipases such C and D (Figure 1.2). Recent studies have implied involvement of cPLA2 in cancer development, though not completely clear [42]. cPLA2 activity initiates inflammation and cell proliferation therefore mutation or alteration of it can lead to cancer [43].

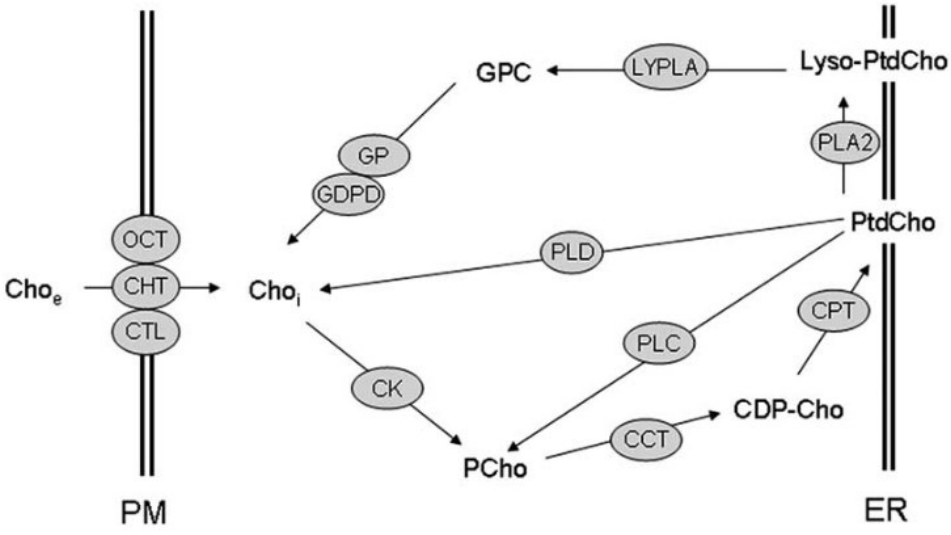

Figure 1.2: Metabolic pathway of choline. Abbreviations: PM – plasma membrane, Cho_e – extracellular choline, OCT – organic cation transporter, CHT – choline high affinity transporter, CTL – choline transporter-like protein, Cho_i – intracellular choline, CK – choline kinase, PCho - phosphocholine, CCT – cytidylyl transferase, CDP-Cho – cytidine diphosphocholine, CPT – choline phosphotransferase, PtdCho - Phospatidylcholine, PLC - phospholipase C, PLD - phospholipase D, PLA2 - phospholipase A2, GPC - glycerophosphocholine, GDPD - lycerophosphodiester phosphodiesterase, ER – endoplasmatic reticulum [44].

1.2.2. **Glucose metabolism in cancer**

In 1924, Otto Warburg a Nobel Laureate described different energy metabolism of cancer cells. Normal cells which experience aerobic conditions, break down glucose into pyruvate in the cytosol through the process of glycolysis, then the pyruvateis broken down further in mitochondria into carbon dioxide in the citric acid cycle (known also as Krebs cycle) [45, 46]. Under anaerobic or hypoxic (low oxygen tension) conditions, normal cells are limited to use only glycolysis, generating pyruvate that is reduced to lactate, which is then secreted from cell. Warburg discovered that cancer cells heavily rely on glycolysis and generating lactate as the breakdown product of glucose even in abundance of oxygen. Later his discovery got name "Warburg effect" [38, 47].

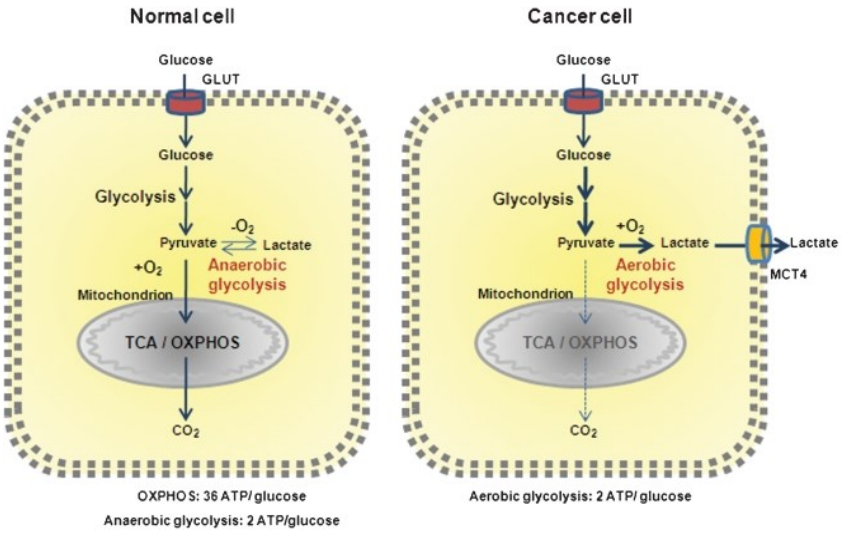

Figure 1.3: Changes in glucose metabolism in cancer cells. In normal cells (picture in left) in the presence of oxygen, glucose enters cytosol through glucose transporters (GLUTs) and then breaks down by glycolysis to pyruvates. Then pyruvates transported to mitochondrion where it completely oxidized to carbon dioxide through tricarboxylic acid (TCA) and oxidative phosphorylation (OXPHOS) process, generating 36 ATPs per glucose. (Right) In the absence of oxygen, pyruvate is metabolized into lactate generating only 2 ATPs per glucose, whereas in cancer cells glucose is mostly converted to lactate regardless to the amount of oxygen (Warburg effect). It is then transported out of the cell through lactate transporter [48].

Aerobic glycolysis (Warburg effect) has been a subject of interest to cancer researchers for many years. The fact that cancer cells use inefficient way to produce ATP even in the abundant presence of oxygen is still under research. One of the explanations comes from the observation that the cancer cells within tumor have often not enough access to oxygen. Hypoxia forces normal cells to glycolysis too, so maybe cancer cells would be more adapted to this condition. In many cases, it was shown that hypoxia contributes to tumor aggressiveness [49]. Even in the presence of enough amount of oxygen, cancer cells anyway use aerobic glycolysis, thus indicates involvement of mutations on glucose regulation genes [50].

The fact that cancer cells metabolize glucose in an ineffective way requires them to countervail by importing large amounts of it into the cells. This makes cancer cells express high levels of glucose transporters, GLUT1, which covers big part of plasma membrane to uptake glucose in enormous amounts [51, 52]. This seemingly inefficient metabolism of glucose on first sight is actually compensating ATP production on the higher rates of glycolysis in general. In addition, high glycolytic rate enables cancer cell to manipulate biosynthetic pathways to produce large amount pf biomass. When it comes to glycolysis product lactate, last findings suggest that lactate as a weak acid transported outside cell, helps to acidify extracellular matrix and activates proteases, which cause matrix degradation and cell detachment. This contributes to cancer cell invasion and metastasis [53-55].

Experimental evidences show that tumor growth is heavily depending on glucose metabolism, and when it is inhibited in one ways or another, tumor growth slows down dramatically. Observations like these provide first indications that the abnormal glucose metabolism in cancer cells can be good target for therapy [56].

1.3. **Animal models in breast cancer studies**

Breast cancer cell lines are important for the *in vitro* studies of cancer, providing information on e.g. gene expression, signaling pathways, or metabolism on cellular level. It also gives good information on different drug sensitivity, but only up to some scale. Breast cancer is a heterogeneous disease and has diverse effect on different tissue in breast and other neighboring tissues. Tumor microenvironment is very important in cancer development [57]. That is why experiments with animals are necessary in characterization of cancer as a biological system and observe cell-to-cell communication in a more natural environment. *In vivo* experiments can show

interactions between cancer cells and their surroundings and their relation to cancer cell phenotypes, response or resistance to treatment and assist in establishment of biomarkers for new cancer treatment [58]. Many breast cancer cell lines were obtained from aggressive tumor types on late stage of metastasis, so they have very different characteristics from other less invasive subtypes. In addition, some breast tumors are not possible to grow as a cell line, due to their short life outside of organism. In such cases, animal models are better choice to grow and observe these tumors.

Animal models cannot completely mimic human organism; that is why there often are different models to study a particular subject of interest. For instance, in preclinical research, tumors develop spontaneously in transgenic animals or grown as xenografts in severe combined immunocompromised (SCID) animals with implanted cancer cells from patients [59]. These models based on transplanted primary patient tumors (PPTT) are good to study breast cancer heterogeneity. PPTT based models in cancer therapy usually show good correlation with patients tumor response to new treatment methods and angiogenesis development [60, 61]. However, transplantation efficiency is low and should be considered careful in regards of transplantation location and other matters [62]. Xenografts are also frequently used for medical imaging studies, because they are quickly to grow and easy to use. These models cannot be used alone for studies of new drugs, due to the lack of immune cells and its response. That is why experimental design should be developed carefully regarding immune system. In many experiments, subcutaneous xenografts grown from patients' tumor tissues have provided relevant information to clinicians, and some cancer cell lines' compatibility with animal models have been thoroughly characterized [63]. Commercial availability of specific experimental models makes it easy to compare results and develop new strategies in research.

In addition, it is better to use several cell lines in model organism to mimic heterogeneity of breast cancer instead of only one cell line [64]. Because breast cancer affects several tissue types and thus has rich genetic variety. To study genetic background of breast cancer in organism genetically engineered mouse models (GEMM) are used. Since mice and humans have similar mechanisms in cancer development GEMM allows studies of tumor initiation and progression in relation to oncogenic signaling. Though these models are widely used in preclinical experiments of new drugs, human organism is complex and too specific for whole comparison of results.

1.4. Phospholipase A (PLA) Superfamily

Cell membrane is a key component in different cell activities like proliferation, cell death, signaling and many more. In all of these processes, phospholipids in membrane are regulated and controlled by various cell processes. Lipid peroxidation is an important ubiquitous process, which happens under certain oxidative conditions. Due to this, phospholipases play important roles in biochemical machinery of the cell [65].

The phospholipase superfamily consists of enzymes which interact with phospholipids and produce fatty acids and other lipophilic substances. They present in almost all analyzed cell types. They also take important role in signaling cascades leading to several events in cells [66]. Phospholipases are divided to four big families, A, B, C and D, which have their own subgroups. They are categorized acording to the specific sites in phospholipids where they cleave. Since phospholipids are huge part of the membrane, phospholipases participate in all its activity; cell metabolism, proliferation, inflamation and cell-cell communication [67].

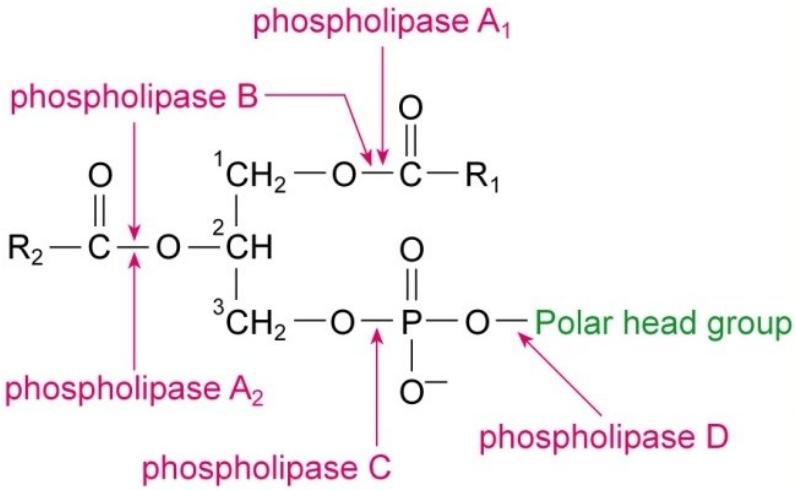

Figure 1.4. Sites on phospholipid where phospholipase superfamily members cleave [68].

There are two main families of PLA: PLA1 and PLA2. They were first purified and charachterized as digestion assistants and strong venom secreted by some snake types. As it is shown in the Figure 1.4., PLA1 cleaves phospholipid on SN-1 position and removes the 1-acyl group while PLA2 removes 2-acyl group from SN-2 position, yielding a fatty acid and a specific lysophospholipid [69]. PLA enzymes usually have high molecular mass around 85kDa and are involved in initiation of inflammatory response.

PLA1 usually act as digestive enzymes and regulate lysophospholipid production. Some studies suggest that some members of PLA1 family are involved in virulence factor and take part in Lands Cycle [70, 71]. Different studies find out involvement of different products of PLA1 catalysis in various processes like platelet aggregation and smooth muscle contraction. PLA1 structure is not well understood yet and needs more studies [72, 73].

1.4.1. **Phospholipase A2 (PLA2) enzymes family**

There are 16 groups of PLA catalytic enzymes and several subgroups; they are based on their biochemical properties and mechanisms [74]. PLA2 has six types: cytosolic PLA2 (cPLA2), calcium-independent PLA2 (iPLA2), secreted PLA2 (sPLA2), platelet-activating factor acetyl-hydrolase (PAF-AH), lysosomal PLA2 (LPLA2) and adipose PLA2 (ad-PLA2). Some of these PLA2 types (especially cPLA2) by releasing AA are associated with many inflammatory conditions like rheumatoid arthritis (RA), asthma, atherosclerosis and different types of cancers [75, 76].

Intracellular cPLA2, iPLA2 and extracellular sPLA2 are best characterized and called “big three”. cPLA2 is a key player in the inflammatory response, iPLA2 is important in membrane homeostasis and energy metabolism, while sPLA2 takes role in different cellular events by modulating the extracellular phospholipid milieus [77]. Free fatty acids and lysophospholipids form through hydrolysis of phospholipids, and may cause membrane disjunction. Free fatty acids and lysophospholipids stimulate inflammation as precursors for active metabolites [78].

The IV PLA2 group consist of four isotypes: cPLA2α, -β, -γ and -δ [76] They are distinguished by different types of lipid modification, calcium requirement and specific substrate. Structure of cPLA2α, which is most common and also the kind we have been focusing on in this study, consist of two parts: N-terminal with calcium dependent lipid binding site or C2 domain and catalytic domain with active site for MAPK phosphorylation [79]. These domains are responsible for cPLA2 regulation and activation. Depending on calcium presence in cytosol, it is able to translocate to membrane. Peroxidation of membrane phospholipids, tyrosine phosphorylation and protein-protein interaction are also involved in cPLA2 regulation [80]. AA can be broken down to prostaglandins (PG) and thromboxane (TX) by Cyclooxygenase (COX) enzyme or to leukotrienes (LT) and lipoxines by Lipoxygenase (LOX) enzyme. LT, PG and TX are eicosanoids signaling molecules involved in control of cell growth, inflammation and other cellular activities [81, 82].

1.4.2. **Cytosolic phospholipase A2 and cancer**

Cytosolic phospholipase A2 (cPLA2) is dysregulated in many types of cancer, and is strongly related to high levels of proliferative eicosanoids, especially prostaglandin E2 (PGE2) that is usually found in tumor cells [83, 84]. PGE2 is a bioactive lipid involved in many cell activities like cell proliferation, apoptosis, angiogenesis, and immune surveillance. Released AA catalyzes PGG2 by cyclooxygenase (COX1/2) which activates PGH2 and this produces prostaglandins PGE2 included [85]. PGE2 is involved in inflammation and induces fever [86].

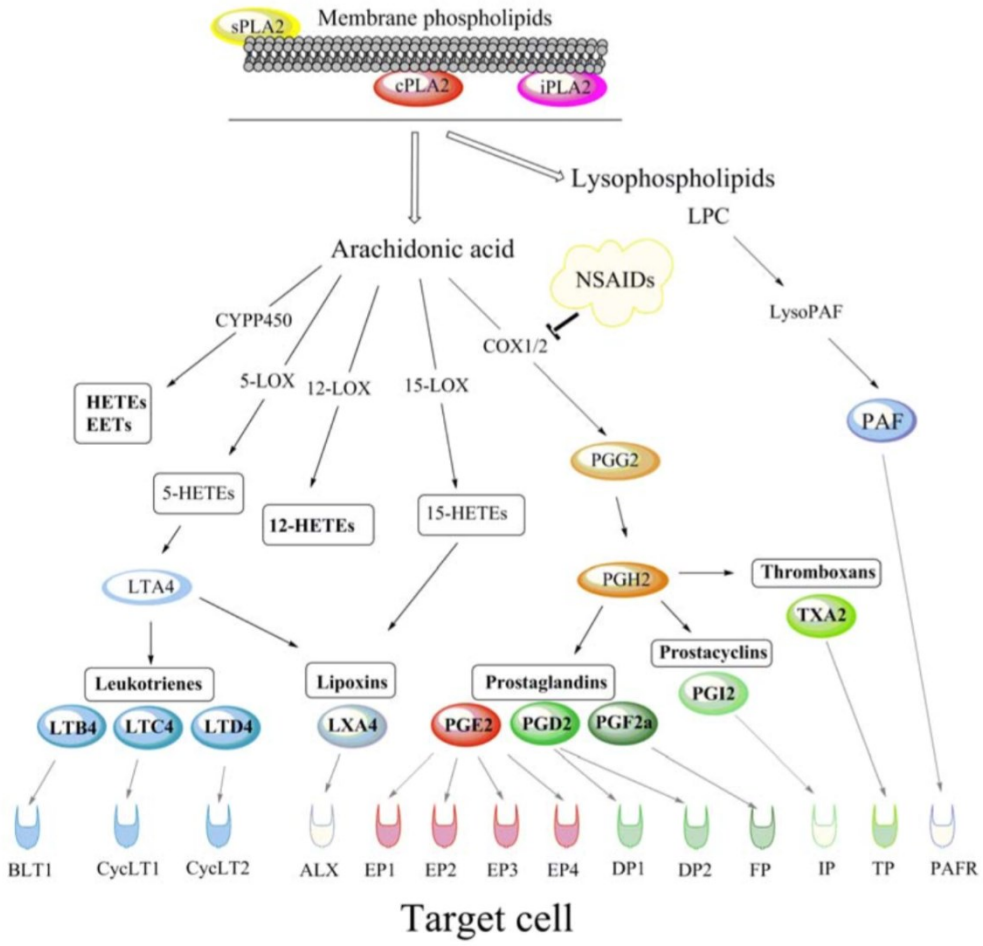

Figure 1.5. Molecular pathway of cPLA2 [87]

cPLA2 are associated with pathogenic diseases too, no surprise due to its inflamatory effect [88, 89]. Alterations in the levels and functional activity of cPLA2 have been associated with different cancers like cholangiosarcomas, prostate cancer, non-small lung squamous carcinoma (NSCLC) and breast cancer. In many of these cancer overexpression of cPLA2 has been reported and often accompanied by cancer associated stimuli EGFR signaling, oncogenic Ras mutations, COX2 and

transforming growth factor beta (TGF-β) overexpression, high level of PGE and secretion of vascular endothelial growth factor (VEGF) [89].

In ovarian cancer studies, high levels of platelet-activating factor (PAF) were observed. PAF is another pro inflammatory lipid mediator, which is activated by a de novo pathway and a remodeling pathway. In de novo pathway levels of PAF are maintained in normal cellular activities, whereas inflammatory agents stimulate remodeling pathway of PAF activation as a pathological response. This process is initiated by cPLA2 hydrolyzing membrane phospholipids and releasing lysophopholipids (LPC) a precursor of LysoPAFs [90].

Another target for cancer therapeutics is angiogenesis, where cPLA2 has been implicated. Lung cancer and glioblastoma are highly angiogenic and resistant to radiation [91]. LPC specifically lysophosphatidylcholine produced by cPLA2 enzymatic activity is converted to lysophosphatidic acid by lysophospholipase D and phosphatidic acid (PA) produced by diacylglycerol kinase is converted to lysophosphatidic acid (LPA) by cPLA2. By involvement of cPLA2 in regulating these potent lipid mediators such as lysophosphatidylcholine, arachidonic acid, and lysophosphatidic acid it accommodates tumor progression and angiogenesis [92, 93]. In following mouse studies inhibition of GIVA cPLA2 with 4-[94]-ethoxy]benzoic acid CDIBA (Morria Biopharmaceuticals plc), showed promising results in the formation of fewer lung tumors and no brain tumors in treated mice compared to control mice [94].

PI3-K/Akt pathway is abnormal and altered in many cancers, which normally regulates mammalian target of rapamycin (mTOR) signaling. This contributes to dysregulation of cell proliferation, growth, differentiation and survival. Some studies report mTOR activity as critical for angiogenesis and carcinogenesis of breast cancer and AA released by cPLA2 is an activator of mTOR1/2 signaling [83, 95]. This all makes cPLA2 possible good target in cancer therapy.

1.4.3. **New targeted treatments: cPLA2 specific inhibitor AVX235**

Asmentioned before, BLBC is a very aggressive cancer type which respond poorly to available targeted therapies. Therefore new drug targets are needed. One of them is promising cPLA2 inhibitor AVX235 (Avexxin AS, Trondheim, Norway).

AVX235 is a thiazolyl ketone (methyl 2-(2-(4-octylphenoxy) acetyl) thiazole-4-carboxylate) which presented good inhibitory effect of cPLA2 activity in previous research. Since it was originally

developed specifically against cPLA2 it was appointed as anti-inflammatory drug. Its inhibitory properties were established by evidence of decrease in cPLA2 key downstream metabolites. In murine study, no toxic effect was observed and efficient inhibition of cPLA2 in arthritis progression in collagen-induced models [96]. It showed reduction up to 40% of three fold of overexpressed PGE2, the downstream product of cPLA2 activity, in animal models.

In another study of AVX235 treatment against BLBC xenograft models showed significant inhibition in tumor growth tumor perfusion and early modification of cancer cell metabolism. This study was initiated to see anti-vascular effect of AVX235 in BLBC models, which led to long-term tumor inhibition. In general AVX235 is promising therapeutic solution for BLBC patients, who have little choice in therapy [97].

1.5. NMR spectroscopy in breast cancer

Rabi first described magnetic resonance imaging in 1938 [98]. Later in 1952 Bloch and Purcell measured nuclear magnetic resonance signals in water [99, 100]. They won Nobel Prize for these phenomenal techniques. Since then nuclear magnetic resonance (NMR) developed well, in 1970s two-dimensional NMR was discovered. In 1977, Damadian performed full body scan of a human and diagnosed cancer for the first time. More recent studies help to elucidate molecular structure on more dimensions and importance of NMR is obvious from further Nobel Prizes like: K. Wütrich in 2002 (chemistry) and P. Lauterbur & P. Mansfield in 2003 (medicine).

Women with breast cancer commonly have X-ray mammography due to its higher availability and lower costs. Usually this is first step in breast cancer diagnostics [101]. MRI uses magnetic fields to create an image of the breast. It counted as more invasive than mammography because of contrast agent injected before screening. Nevertheless, MRI is better suited for diagnostics and monitoring of cancer. It has various available image contract techniques and better resolution. Combination of PET/CT and PET/MR are specifically developed imaging systems for complementary information and more accurate diagnostics [102].

Nuclear Magnetic Resonance (NMR) in clinics can be used to examine biological tissues or biopsies from patients for metabolite analysis. This method analyzes samples in high field spectrometers. Since in NMR, sample analysis information about localization of different metabolites is not necessary, it gives high quantitative, nondestructive and nonselective results

[103]. NMR can detect abnormal Choline (Cho) metabolism in breast cancer and other cancer types. In normal breast tissue, Cho peaks in NMR spectra is not found, but in examined breast cancer tissue some Cho containing compound peaks like glycerophosphocholine (GPC) or phosphocholine (PC) can be detected [104]. Size of observed tumor matters in sensitivity of NMR in diagnostics [105]. High Resolution (HR) NMR is a technique with enhanced spectra resolutions, which provides optimum conditions for chemical analysis of cell extracts and culture medium for metabolomics studies in cancer research or observing drug treatment. It is often used for analyses of serum and urine where spectra different derivatives of some metabolomes can cluster into peaks together [106].

1.5.1. **Principles of Nuclear Magnetic Resonance**

Magnetic Resonance Spectroscopy (MRS) is based on nuclear magnetic resonance phenomenon. MRS is an analytical technique that can give information about molecules on their chemical, physical and electronical structure. NMR is physical phenomenon when nuclei in magnetic field absorbs electromagnetic radiation and then re-emits it. Analytic method of NMR exploits magnetic properties of specific atomic nuclei such as ^{1}H, ^{13}C, ^{19}F, ^{15}N and ^{31}P in magnetic fields. These nuclei have non-zero spin or odd number of protons and neutrons, and have intrinsic magnetic moment. In the absence of external applied magnetic field $\mathbf{B}_0$ nuclei spins randomly with a magnetic angular momentum μ. Each element and isotope has unique μ. When external magnetic field $\mathbf{B}_0$ is applied, the nuclei will orient spin parallel or anti parallel to the magnetic field. Because the angular momentum is quantized, only certain spin angles are possible. Atoms spin only up or down in the field. The up spin have the lowest energy state. Because most of the nuclei will spin up, net magnetization $\mathbf{M}_0$ will appear [107]. Figure 1.4 shows it.

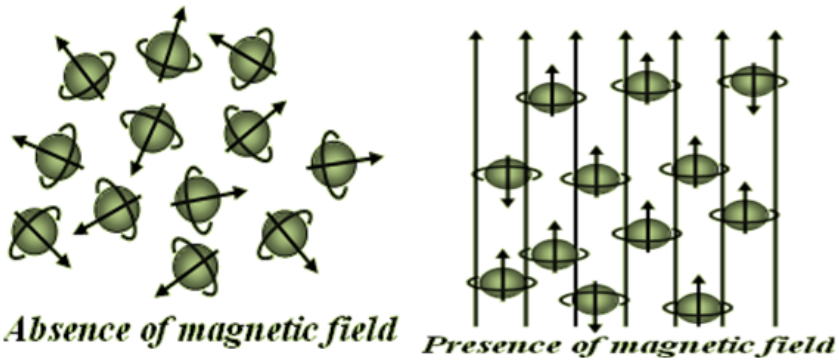

Figure 1.6: Spin orientation of nuclei in magnetic field. Nuclei spin to different orientations in the absence of external magnetic field $\mathbf{B}_0$. Applying this external magnetic field $\mathbf{B}_0$ creates magnetization $\mathbf{M}_0$. Since most of nuclei have low energy state, they align parallel to magnetic field and few anti parallel [108].

These resonance properties are used in NMR spectroscopy for measurements. When radiofrequency (RF) pulse applied to the static magnetic field in a direction perpendicular to external magnetic field and at a frequency that exactly matches the precessional frequency (Larmor frequency) of the nuclei, absorption of energy will occur and nuclei will flip from its lower to high energy orientation (up and down). When RF pulse is turned off, the nuclei flips back or relaxes to equilibrium in longitudinal T1 and transverse T2 manners. This emitted energy Free Induction Decay (FID) of all nuclei versus time is detected and Fourier transformed (FT) to frequency domain as NMR spectra. Figure 1.5 illustrates this transformation. Longitudinal relaxation T1 is the time required to for a system to its original alignment with magnetic field B0 after RF pulse applied. It depends on nucleus type and environment like field strength, temperature, solvent conditions, and presence of macromolecules or paramagnetic ions. Large molecules like lipids or proteins, because of the slow proton exchange movement have short T1. Small molecules have lower possibility for interaction because of their fast movement that is why they have longer T1. Transverse relaxation T2 is the time required for spinning nuclei to lose their phase coherence. Similar to T1, environment where nuclei interacts effects T2.

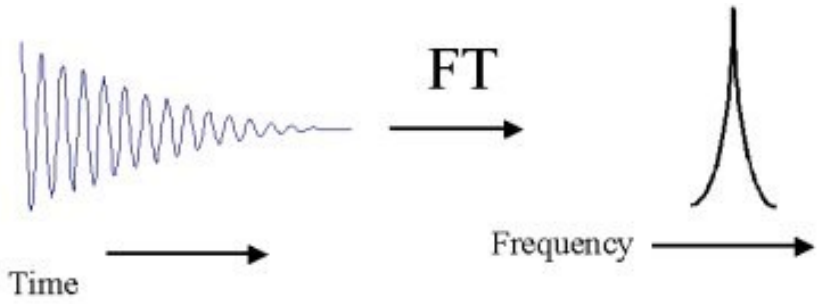

Figure 1.7: Transformation of FID to frequency. Free Induction Domain (FID) in the time domain Fourier Transformed (FT) to Frequency domain Hz [108].

Atomic nuclei are shielded by electron density differently according to the different molecular environment. Thus, it gives different chemical shift of a nucleus, which influences electron distribution. Difference between the resonances are very small and chemical shifts are expressed as parts per million (ppm) on NMR spectra. Different substances like methyl groups, double bonds and aromatic rings have similar bonding situation of ^{1}H resonance and they group together

on NMR spectrum. They also influence each other by spin coupling and cause splitting of single peaks into multiple peaks depending on number of protons. Because all of these different molecules (metabolites) can be detected and identified by looking at the chemical shifts and coupling interaction (splitting patterns) and relative signal intensities, which are unique for each metabolite. Intensity of signal can be calculated by using appropriate reference calibration standards [109, 110].

1.5.2. ^{13}C NMR and ^{1}H NMR

NMR is well adapted for metabolomics researches because it quickly and qualitatively provides unbiased detection of small metabolites. Given same conditions of chemical environment and temperature, metabolites will always appear at the same peak on NMR spectrum. HR MRS provides limited characterization of several metabolites on 20 ppm chemical shift range despite high-to-signal ratio (SNR). In this connection ^{13}C NMR has larger scale of chemical shift up to 250 ppm. This gives better separation and characterization of metabolite peaks. Since natural ratio of ^{13}C is around 1.1%, the inherent sensitivity is so low that it is difficult to detect metabolites only through naturally abundant ^{13}C nuclei for SNR distinction. In addition to sensitivity, the incubation approach allows us to evaluate the rate of consumption and conversion. That is why this technique requires already labeled ^{13}C isotopes in procedure. Eakin and Morgan first used ^{13}C in NMR studies in 1972, it was expanded to other types organisms like cells, organs, animals and humans [111, 112].

Due to the altered glucose metabolism in cancer cells, ^{13}C labeled glucose is often used in NMR to study cancer metabolism. In these experiments ^{13}C labeled glucose helps to track metabolic pathways like glycolysis, glutaminolysis, Krebs cycle etc. in samples and see final derivatives of glucose metabolism. In our project, we used ^{13}C labeled glucose to see effect of AVX235 and the PI3K inhibitor BEZ235 on MDA-MB-231 breast cancer cell line [113].

As we described before, altered glucose metabolism is cancer trait (Warburg effect). When ^{13}C labeled glucose is added to cancer cells glucose free media, then it is possible to trace how labeled glucose converted to labeled pyruvate through glycolysis. ^{13}C labeled pyruvate then can be converted to amino acids like glycine and alanine, or it can enter TCA cycle and produce glutamate, or converted directly to lactate. All of these products are labeled by ^{13}C and can be found on NMR spectrum. Figure 1.6 illustrates this process [114, 115].

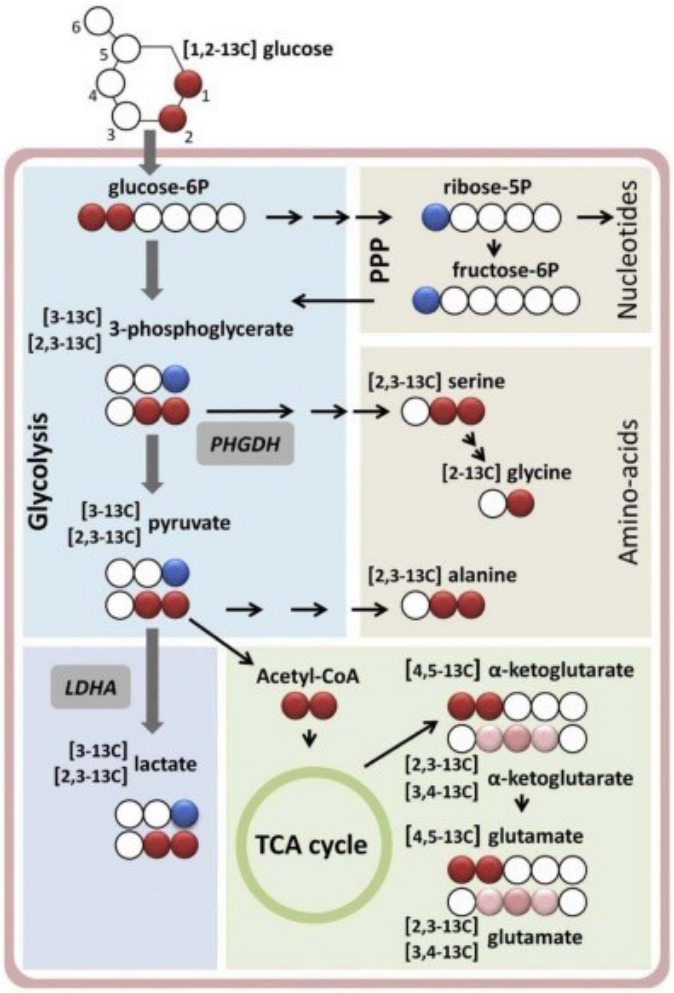

Figure 1.8: ^{13}C labeled glucose metabolic pathway. 1,2-^{13}C labeled glucose undergoes glycolysis and Pentose Phosphate Pathway (PPP). Then it goes either to glycolytic metabolism-linked biosynthesis of amino acids or to Tricarboxylic Acid (TCA) cycle. Circles representing carbons, red circles are labeled ones, blue circles are showing conversion through PPP and glycolysis, and pink circles indicate that 50% or less of that molecules in that position are formed of labeled ones [114].

Previous studies using ^{13}C labeled glucose showed good efficiency in establishing metabolic players like ^{13}C labeled lactate and glutamate in cancer. By providing broad results, ^{13}C NMR is good technique in diagnostics and cancer treatment monitoring [116, 117].

^{1}H NMR spectroscopy or proton NMR is another technique to determine structure of molecules with regard to hydrogen-1 nuclei. Usually deuterated (containing deuterium, ^{2}H) solvents are used as reference e.g. deuterated water (heavy water) with small amount of tetramethylsilyl (TMS) for calibrating chemical shifts. Chemical shift range of ^{1}H NMR is in between +14 and -4 ppm range. ^{1}H NMR provides abundant amount of information of quantitative and qualitative

character. Because of this, multivariate statistical analyses is used to process data from just one experiment [118].

While ^{1}H NMR can provide metabolic fingerprint of analyzed samples, ^{13}C NMR can provide metabolic flux information. ^{1}H NMR is limited to the smaller range of chemical shift ppm with more detailed spectra and it is water intolerant (gives weaker peaks) compared to ^{13}C NMR. Unfolded proteins give wider distribution on spectra in ^{13}C NMR. Another disadvantage of ^{13}C NMR that it has slower T_2 relaxation and requires longer repetition-delay, more time [119].

2. **OBJECTIVES**

Abnormal metabolism in cancer cells is one of the hallmarks of the cancer which makes metabolism a good target and possible biomarker for new pharmaceutical drugs. Previous studies of AVX235 showed promising results as anti-inflammatory agent and anti-vascular effect on patient-derived BLBC models [96, 97]. Based on these results, the main objective of this research was to investigate the effect of AVX235 on basal like breast cancer cell line. More specifically, the objectives of the project were to:

- Identify if AVX235 exerts cytotoxic effects on mda-mb-231 cells
- Examine how cPLA2 inhibition by AVX235 is reflected on altered metabolic profile in breast cancer cells
- See if AVX235 influences cellular consumption and utilization of glucose

3. MATERIALS AND METHODS

3.1. Histopathology and mitotic cell counting

The objective of this experiment was to evaluate effect of AVX235 in tumor cells obtained from patient-derived basal-like breast cancer models. In clinical medicine, histopathological samples of tissue are gathered from patients or animals by biopsy or small surgeries for microscopic observation.

In this study MAS98.12 patient derived BLBC and TNBC xenograft models were set and maintained. Patient derived tumors were bilaterally implanted into the thoracic mammary fat pads of female Hsd:Athymic Nude-Foxn1^{nu} mice and prepared for experiments. Mice were kept in pathogen-free environment Housing conditions were: room temperature 19 ^{o}C – 22 ^{o}C, humidity 50%-60% and 12 hours light/dark cycle. Diet included RM1 (Scanbur BK, Karlslunde, Denmark) and distilled water ad libitum. Mice were divided to a treatment and control groups when diameter of tumor reached ~6 mm. Treatment group received 30 mg/kg AVX235 dissolved in 50 µL of 100% DMSO and control group received only 50 µL of 100% DMSO by daily intraperitoneal (i.p.) injections for 2 days (n = 6 for each group) and for 5 days (n = 5 for each group). Animals were weighed twice a week and daily checked. In the end of the experiment animals were killed by cervical dislocation and immediately after the excision, tumor was preserved in formalin.

The NTNU Cellular and Molecular Imaging Core Facility provided the histological staining. Samples obtained from mice were sliced to small sections, around 4 um in thickness and immediately fixed on glass slides permanently, then they are stained with different dyes [97].

Samples were stained with lectin (*Griffonia simplicifolia* lectin I, Vector Laboratories, Burlingame, CA, USA) and anti-Ki67 (monoclonal rabbit anti-human Ki67 with cross-reactivity to mouse; Abcam, Cambridge, United Kingdom), hematoxylin and eosin (H&E kit, Mayer's Hematoxylin Solution - 250ml and Eosin Solution - 250ml) and phosphohistone H3 (PHH3, Serine 10) stains. HE stain is a gold standard dye that stains nuclei with its other components to blue and eosinophilic structures to pink, lectin is carbohydrate-binding protein usually used for staining of endothelial cells to blue, anti-Ki67 is a proliferation marker stains nuclei of mitotic cells to brown and PHH3 stain is another proliferation marker which stains histones in mitosis to brown. Lectin and anti-Ki67 were used together in double staining.

Each slide was observed under 40X magnification with Olympus BX41TF (Olympus America Inc., Melville, NY) microscope. Ten observation fields (hot spots) were chosen diagonally across the whole slide and all mitotic cells in each field were counted. Numbers of mitotic cells were recorded for each slide separately and images were taken. Student's *T*-test was employed to check for significant differences between the groups ($\alpha = 0.05$).

All experiments with animals were carried out according to the European Convention for the Protection of Vertebrates used for Scientific Purpose and with approval of National Animal Research Authority in Norway.

3.2. **Cell experiments**

One of the benefits of using cell lines in experiments is that they give relatively homogeneous cell population, are easy to replenish, and have good reproducibility. The MDA-MB-231 is one of the oldest and well-studied cell lines. They are easy to grow and have simple metastatic model. Morphologically they can change from spherical shapes to spindle shapes. This is observable under microscope as indicator of some stress, so cells tend to stretch to each other to cover maximum surface and easily communicate [120]. MDA-MB-231 cells are triple negative breast cancer cells.

MDA-MB-231 cells in our research were obtained from American Type Culture Collection (ATCC). The cells were kept in liquid N2-tank in ampoules. On the day of experiment they were thawed with suggested protocol from ATCC and prepared for further use [121]. The cells were cultivated and maintained in 25cm^2 (T25) vented flasks from Sarstedt in the beginning, so cells can growth faster, and then transferred to 75cm^2 (T75) vented flasks for growing until growth experiments.

The cells were maintained in a humidified incubator at 37°C with 5% CO_2 and split at sub-confluent state every 3-4 days in a sterile cabinet called LAF-cabinet. Cells were counted and 1000 000 cells were transferred to the cultivation flask each time cells were split. The cells were split by washing the cells 2 times with 10 ml PBS in room temperature, adding 1.5 ml of preheated (37°C) 0.05% Trypsin EDTA and incubating the cells for 4-5 minutes at 37°C. To loosen the cells from the surface of the flask, the flask was gently tapped against the lab bench. Trypsin was deactivated by adding DMEM supplemented with 10% Fetal bovine serum (FBS) approximately 4x the volume of trypsin. The solution was then transferred to a 15 ml centrifuge tube and centrifuged at 700 rpm at 25°C for 5 minutes. After centrifugation, the supernatant was discarded and cells were re-suspended in fresh growth media to the needed ratio. The cells were

counted by using Bürker chamber and recorded in lab book. Cells were transferred to a tissue flask with 9 ml fresh preheated (37°C) DMEM 10% growth media with Gentamicin and incubated thereafter in a humidified 5 % CO_2 incubator at 37°C.

3.2.1. **Cell growth experiments**

12 T25 cultivation flasks with 5ml of fresh 10% DMEM medium were prepared. Procedure from above was done until the splitting part. 320 µl of cell resuspension were added to each T25 flask and incubated in a humidified 5 % CO_2 incubator at 37°C.

Every day 2 flask from 12 were used for counting. Cell confluency was recorded. The cells were washed 2 times with 10 mL PBS in room temperature, 0,75 ml of preheated (37°C) 0.05% Trypsin EDTA added and incubated at 37°C for 4-5 minutes. To loosen the cells from the surface of the flask, the flask was gently tapped against the lab bench. Trypsin was deactivated by adding DMEM medium with 10% FBS approximately 4x the volume of trypsin. The solution was then transferred to a 15 mL centrifuge tube and centrifuged at 700 rpm at 25°C for 5 minutes. After centrifugation, the supernatant was discarded and cells were re-suspended in 2ml of fresh growth media. 10 µl of cells suspension were taken on slide, counted by using Bürker chamber and recorded in lab book. Remaining flasks with cells were freshened with new media.

This was repeated every day to observe cell growth. Population doubling time (PDT) was calculated from the average of counted cell numbers every day.

3.2.2. **MTT assay**

MTT assay measures metabolic activity of cytoplasmic enzymes and shows cytotoxicity of drug as altered viability of the treated cells. Normal viable cells produce NAD(P)H-dependent cellular oxidoreductase enzymes in their mitochondria, which can bind to tetrazolium dye MTT 3-(4,5-dimethylthiazol-2-yl)-2,5-diphenyltetrazolium bromide and produce new purple compound formazan (crystal formation). It is observable with eyes. Therefore, MTT assay is colorimetric assay, which can give qualitative data, but by measuring intensity of purple color with spectrophotometer at certain wavelength, it can also provide quantitative data too. Our purpose

was to find IC50 for AVX235 in different breast cancer cell lines (MDA-MB-231, MCF-7, SKBR3). To see effectiveness of AVX235 in inhibition cPLA2 activity.

Cells were grown the way we did in part 3.2. and on experiment day were plated on 96-well plates in triplicate columns for each cell line. For each row 100ul of different concentration of AVX235 were added. Serial dilutions from 60 uMAVX235 stock (Prof. George Kokotos, University of Athens) in regular serum-free DMEM was made. As a control DMSO volume-matched to the highest AVX235 concentration was included.

Layout: Cell lines in triplicates (vertically).

A - 0uM	MDA-MB-231	MCF-7	SKBR3
B - 5uM	MDA-MB-231	MCF-7	SKBR3
C - 10uM	MDA-MB-231	MCF-7	SKBR3
D - 15uM	MDA-MB-231	MCF-7	SKBR3
E - 30uM	MDA-MB-231	MCF-7	SKBR3
F - 40uM	MDA-MB-231	MCF-7	SKBR3
G - 60uM	MDA-MB-231	MCF-7	SKBR3
H - 10% FBS	10% FBS	10% FBS	10% FBS

The cells were then incubated in a humidified incubator at 37°C with 5% CO_2 according to the standard culture procedure for 24 hours.

Next day MTT solution from 1ml of MTT in 9ml of DMEM was made. 100ul of diluted MTT solution were added to each well. Then the plate was incubated in a humidified incubator at 37°C with 5% CO_2 for 4 hours. MTT is light sensitive, so light exposure was minimized.

After 4-hour incubation MTT solution and DMEM, media of cells were aspirated from wells and 100ul of DMSO was added to dissolve formed formazan crystal. Then plate was shaken on shaker at 150 rpm for 5 min. Absence of formazan crystals were observed in a light microscope. If presence of formazan was observed then the plate needed more shaking. After that plate was read on plate reader at 550-590nm.

3.3. **13C Glucose experiments**

The purpose of this experiment was to evaluate the effect of AVX235 on the overall metabolic profile of breast cancer cells and to see how AVX235 influences the consumption and utilization of glucose. 1,2-13C labeled glucose makes it able to follow the derived molecules down the various metabolic pathways, as this labelled carbon can be distinguished from other carbon isotopes in the sample.

For ^{13}C Glucose experiments MDA-MB-231 cells were grown in same way as in part 3.2. When cells reached confluency of 90 % in T175 flask (around 10-12 million cells) experiments started. ^{13}C glucose media was prepared by adding 0.5 gr of labeled ^{13}C glucose in 25 ml of glucose-free DMEM media to make stock solution of 20 g/L (10X solution). 10µM AVX235, BEZ235 and DMSO concentrations were prepared in ^{13}C glucose DMEM media (1X). Cells in 3 T175 flasks (around 10-12 million cells) with labeled ^{13}C glucose media were treated with AVX235, BEZ235 and DMSO, then incubated in a humidified incubator at 37°C with 5 % CO_2 for 6 hours.

After 6 hours, media in each flask were gathered separately in 50 ml tubes. Cells were immediately washed with cold 10ml PBS. Flasks were scraped for remaining cells with 6 ml (then 4 ml for extra scraping) cold PBS and collected in separate 15 ml centrifuge tubes. 10 µl of cells in PBS were taken to count by using Bürker chamber and results were recorded. Then cells in tubes were centrifuged (1200rpm, 4 ^{o}C for 5min) and supernatant were collected to be aliquoted into smaller Eppendorf tubes. Cells in pellets were re-suspended with 1 ml cold PBS. Remained pellets were centrifuged (1200rpm, 4 ^{o}C for 5min), supernatant collected separately into smaller Eppendorf tubes pellets re-suspended with 1 ml cold PBS. This was done two times. Remained pellets with PBS were shock freezed in liquid N2. Cell pellets and supernatant were stored in Eppendorf tubes in -80 ^{o}C for later use.

Later cell pellets were thawed on ice for 5 min. 750 µl of pure EtOH were added on top of the cells and mixed (vortexed). Then tubes were centrifuged (18000 rpm, 4 °C for 15 min) and supernatant were collected. This was done two times. Supernatants (metabolite extraction) were combined. Then cell extracts were vacuum dried and stored in -80 ^{o}C for NMR analysis

3.4. NMR Spectroscopy

Freeze-dried cell extracts were dissolved in 600 µl of PBS/deuterium water (D2O) buffer with 1mM trimethylsilyl propionate (TSP) as a chemical shift reference, then vortexed well until all solid parts were dissolved and sample was transparent. Then 550 µl of this diluted sample was transferred to standard 5mm NMR tube (Bruker Biospin GmbH, Germany) for spectroscopy analysis. NMR spectra experiments were performed in MR lab with Bruker Advance III Ultrashielded Plus spectrometer (Bruker Biospin GmbH, Germany). The spectrometer was equipped with a 5mm QCI Cryoprobe with integrated cooled preamplifier for ^{1}H, ^{2}H and ^{13}C. One-dimensional (1D) proton spectra were acquired., using a 1D NOESY (Bruker: noesygppr1D) experiment. 13C spectra were acquired with power gated coupling sequence with a 30^{0} pulse angle (Bruker: zgpg30).

Experimental parameters of NMR spectra:

NMR pulse sequence	^{1}H NOESY (noesygppr1D)	^{13}C zgpg (zgpg30)
Temperature (^{0}C)	6	6
Number of scans	256	32768
Time domain (TD)	65536 data points	98304 data points
Acquisition time (s)	2.65	1.65
Sweep width (ppm)	20.5682	197.15

3.5. NMR Spectroscopy data analysis

NMR spectra provides huge amount of data and requires complex analysis. For this purpose computational tools are necessary. Multivariate analysis is good tool (PCA in our case) and can handle several statistical variabilities at the same time. It can operate automatically and consider all conditions you set. NMR spectra requires preprocessing for setting all factors in data to make results qualitative.

Principle component analysis (PCA) is a descriptive and exploratory method. It reduces the original variables into a lower number of non-correlated factors; it visualizes this correlation into linear combinations of variables and visualizes proximities among statistical units. These linear combinations are called principal component (PCs). PCA has many principal components, but usually first few are most important, showing large variance in the data [115].

In our experiments, PCA (multivariate analysis) was performed on ^{1}H spectra to discriminate samples of DMSO (controls) vs AVX235-treated vs BEZ235-treated. Data set was created in MATLAB and all spectra were assigned to correct titles. Baseline was corrected to remove distortion that can change real peak intensity values to avoid inaccuracy in quantification of metabolites. All spectra were corrected to same baseline and were manually phased and TSP was referenced to 0 ppm. Other ppm labels assigned and cleaned up the noise regions and water, to make samples comparable to each other. Range of cleaned data on spectra is between 0.5 ppm to 4.5 ppm. After baseline was normalized, spectra of samples were aligned to perform principle component analysis with aligned data (Figure 3.8.). Peak alignment were done by algorithm of interval correlated shifting Iconshift. 4 hours PCA was performed with aligned data.

Also personal calculation of metabolite peaks on ^{1}H and ^{13}C NMR spectra were performed. In order to evaluate accurate amount of metabolite production, prominent peaks were integrated. Obtained value from integration was divided by cell numbers of that sample.

4. RESULTS

4.1. Histopathology

In order to evaluate the effect of AVX235 on proliferation, tumor samples from control and AVX235 treated mice were sectioned and stained with a lectin/anti-Ki67 double stain (Fig. 4.1, left) and anti-phosphohistone H3 (PHH3; Figure 4.1, right). The lectin will stain endothelial cells, while Ki67 is a marker of proliferation. Coinciding staining implies proliferating endothelial cells. PHH3 is a marker for mitotic nuclei.

One slide per tumor was examined as described in part 3.1 with results given in tables 4.2. and 4.3. Treatment with AVX235 did not give any significant differences after two or five days.

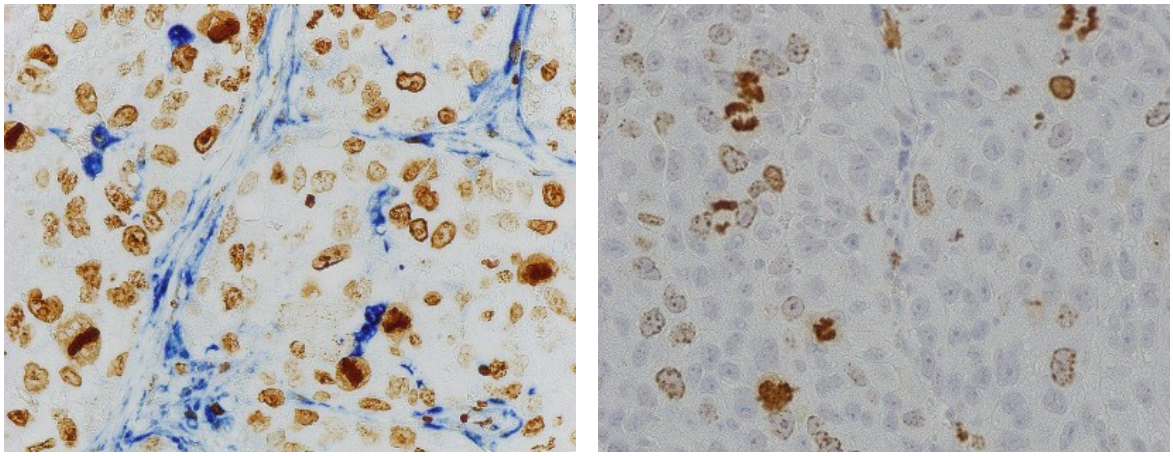

Figure 4.1. Left: Example of lectin/anti-Ki67 staining. Lectin stain for endothelial cells in blue and anti-ki67 stain as proliferation marker in dark brown. **Right:** Example of PHH3 staining. Histones of cells in mitosis stained in brown.

Mitotic cell counting:

Table 4.2. Average number of proliferating and mitotic cells per slide in 2 and 5 day groups of control and AVX235 treated samples with standard deviation.

	ki67		PHH3	
	Cells average	SD +/-	Cells average	SD +/-
2day control	11.14	4.37	13.34	4.33
2day treated	11.12	5.42	13.78	3.35
5day control	11.09	3.91	8.77	2.49
5day treated	11.59	4.11	9.15	2.34

Table 4.3. Statistical analysis of *p*-value of 2 and 5 day groups. With PHH3 showing significan decreace in mitotic cells on 5 day samples in comparison to 2 day samples.

	2d control/2d treted	2d control/5d control	5d control/5d treted	2d treated/5d treated
ki67	0.99	0.96	0.71	0.77
PHH3	0.78	0.01	0.55	0.01

50 slides in total were observed and counted for proliferating cells under microscope with 40X magnification. For each staining of lectin/anti-Ki67 and PHH3 this includes 5 slides per 2 day control and 2 day treated groups, 7 slides for 5 day control and 8 slides for 5 day treated groups. To find out whether there is significant difference between control group in comparison to AVX235 treated group for 2 and 5 days, Student's t-test were applied and *p* value calculated. All *p*-values showed $p > 0.05$ except PHH3 5 day.

4.2. Cell growth curve

In order to see growth rate of MDA-MB-231 cell line, 6 days growth experiment was performed. Cell growth curve was produced from the results of it. Population doubling time (PDT) is approximately 30 hours.

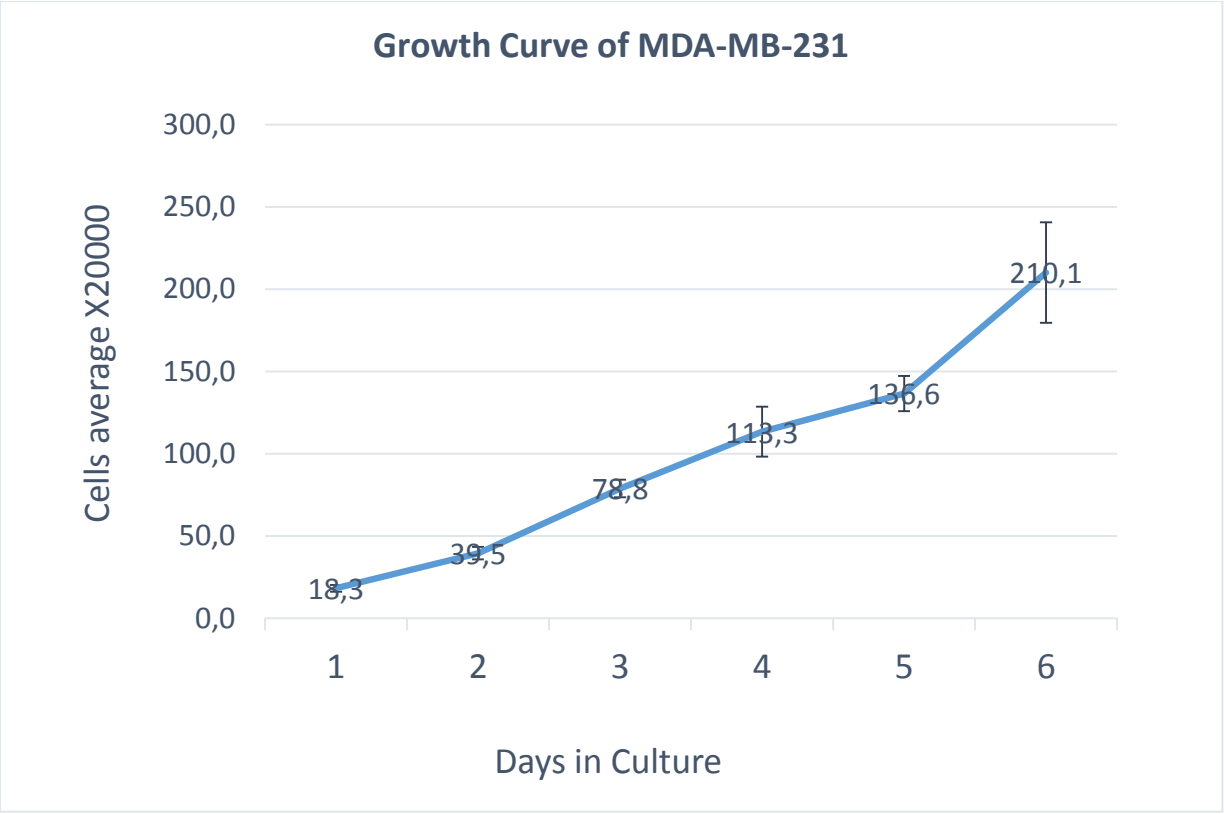

Figure 4.4. Curve of MDA-MB-231 cell line in six days. Y-axis indicates cell numbers reported as mean +/- SD in 2 ml DMEM medium. Bars indicate standard deviation.

4.3. MTT assay

MTT assay was performed to see cytotoxicity effect of different concentrations of AVX235 on MDA-MB-231, MCF-7 and SK-BR-3 cell lines. Three different breast cancer lines showed similar results. MDA-MB-231 cells showed slight increase in viability at low concentrations of AVX235. While MCF-7 and SK-BR-3 cells showed immediate effect of viability decrease in lower concentrations of AVX235, though not so big. 40 µM and 60 µM of AVX235 showed high toxicity on all cells.

Half maximal inhibitory concentration (IC50) values of MDA-MB-231, SK-BR-3 and MCF-7 cells were identified through calculation with sigma plot prgram (Figures 4.4). Different types of breast cancer cells were chosen to see effect of cPLA2 inhibition in luminal like HER2 (-) cells and HER (+), along with triple-negative breast cancer cells. The viability was calculated from OD-values by setting DMSO controls to 100 %. Then standard curves were fitted to the data points using Sigmaplot 13.0, while AVX235 concentrations are fixed. MDA-MB-231 cells' graph showed abrupt

decline of curve at 28 µM concentration of AVX235. On the other hand MCF-7 and SK-BR-3 cells' graph showed more gradual decline of curve.

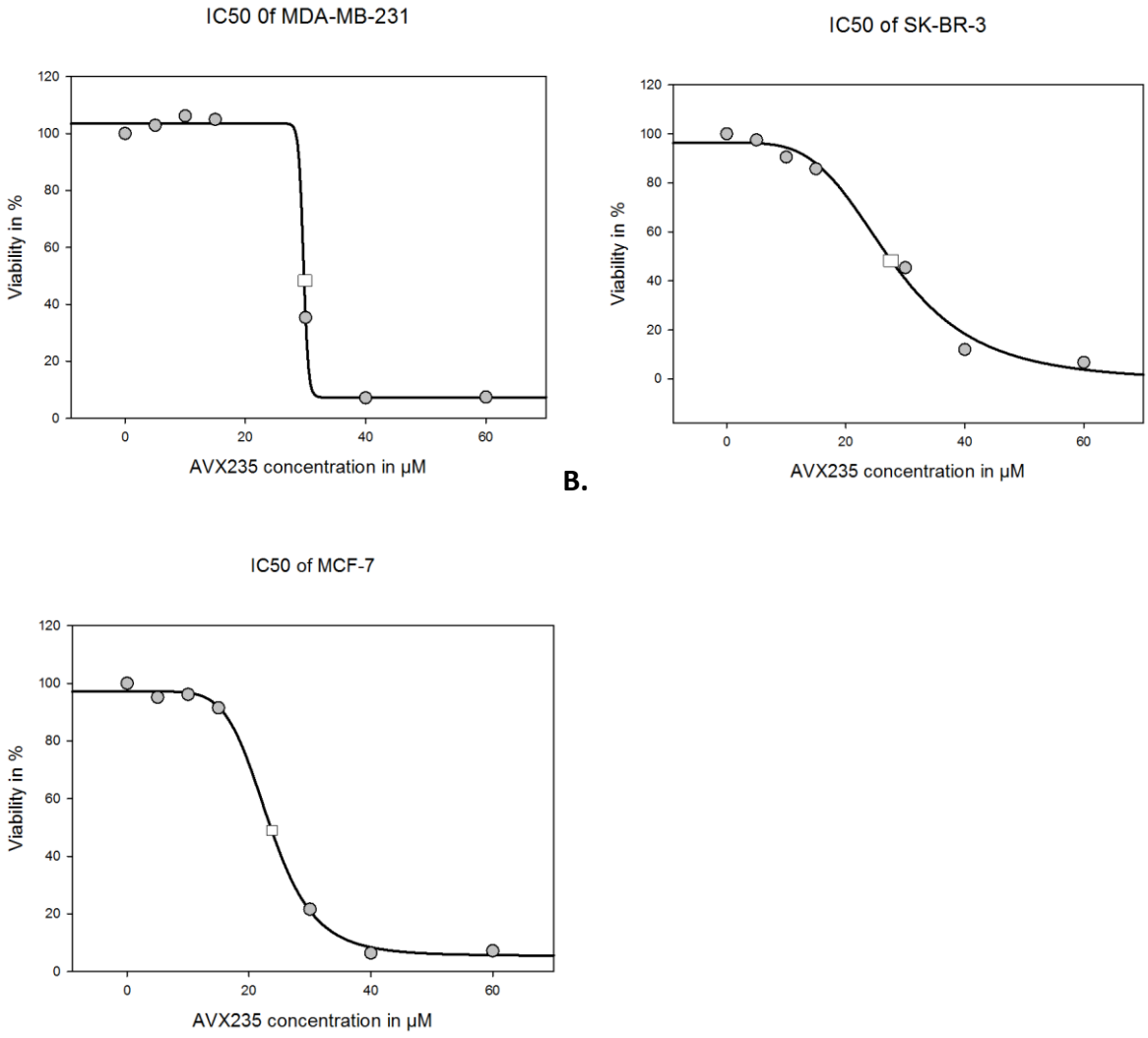

Figure 4.5 (A) Effect of AVX235 concentration of MDA-MB-231 cells, **(B)** SK-BR-3 and **(C)** MCF-7 cells viability measured with the MTT assay. Grey dots indicate measured viability percentage on 0, 5, 10, 15, 30, 40 and 60 µM concentrations of AVX235. White square box shows 50% of survival for MDA-MB-231 cells at 29.7 µM, for SK-BR-3 cells at 27.1 µM and for MCF-7 cells at 23.6 µM concentration of AVX235.

4.4. ^{1}H NMR spectra

In order to examine metabolite profile of breast cancer cells in response to treatment with AVX235 1H and 13C NMR spectroscopy was applied. 10 µM of AVX235 were used due to the less

toxicity effect and according to previous studies [96]. In total 12 MDA-MB-231 cell extract samples were analyzed through 1H NMR and spectra were obtained. 1H spectra of cell extract revealed the profile of various metabolites as demonstrated in figure 4.6. All observable peaks on 1H spectra were identified and labeled for further analysis. Most prominent choline spectra standard peaks at 3.2 ppm were used to verify peaks assignment. Some contamination on spectra 3.7 ppm was detected. Noesy 1d was used. All spectra were aligned and compared in figure 3.8.

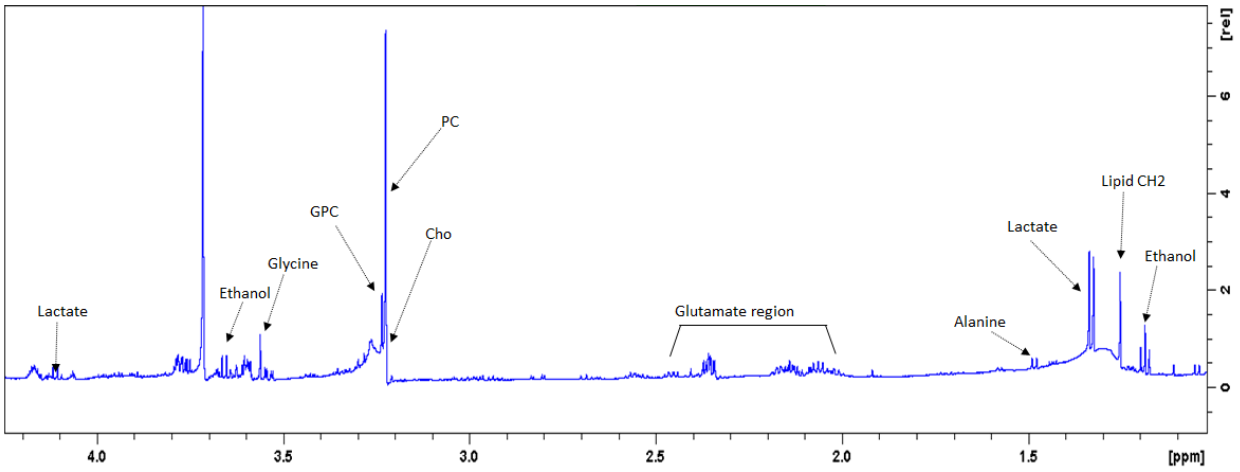

Figure 4.6. Mean spectra of the input data (noesygppr1d), zoomed from 1 ppm to 4.2 ppm. The assigned peaks are lactate, ethanol, glycine, glycerophosphocholine (GPC), phosphocholine (PC), choline (Cho), glutamate region, alanine and lipid CH2.

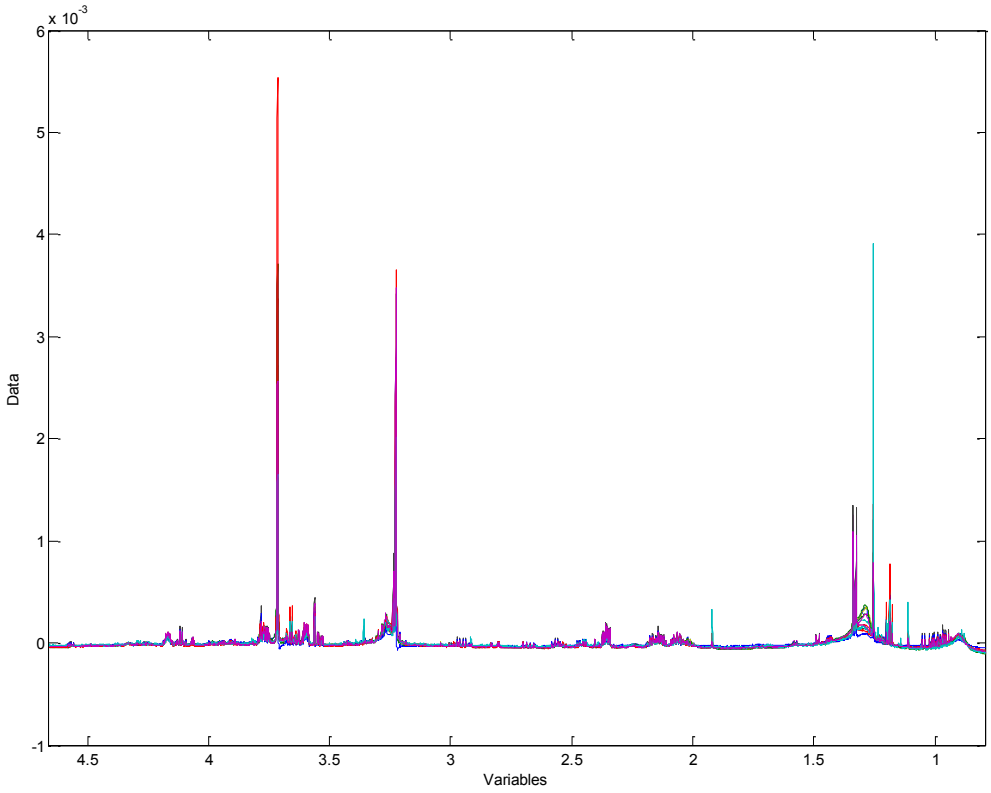

Figure 4.7. Baseline normalized and spectra of DMSO (controls) vs AVX235-treated vs BEZ235-treated samples aligned. DMSO - red, BEZ235 - blue and AVX235 - purple.

In order to map metabolite profile of MDA_MB-231 cells in response to AVX235 and BEZ235 treatment a PCA was performed based on ^{1}H NMR spectra of cell extracts. Figure 4.8 shows bi-plot from PCA based on metabolites formed in choline pathway. Half of the AVX235 and BEZ235 treated samples clustered in the bottom part of the score plot with low PC2 score and the other part near mean line. DMSO samples showed high variability with different results.

Excluding all DMSO controls and performing a PCA of the BEZ235 vs AVX235 treated group's spectra shows a separation between them (Figure 4.9). Bi-plot showed separation with majority of BEZ235 treated samples below mean and majority AVX235 treated group over mean. This was reflected in spectra in figure 4.10, where dots in purple indicate PC3 in lactate differences at 1.3 ppm and 4.1 ppm peaks. BEZ235 treated cells have more lactate than AVX235 treated cells.

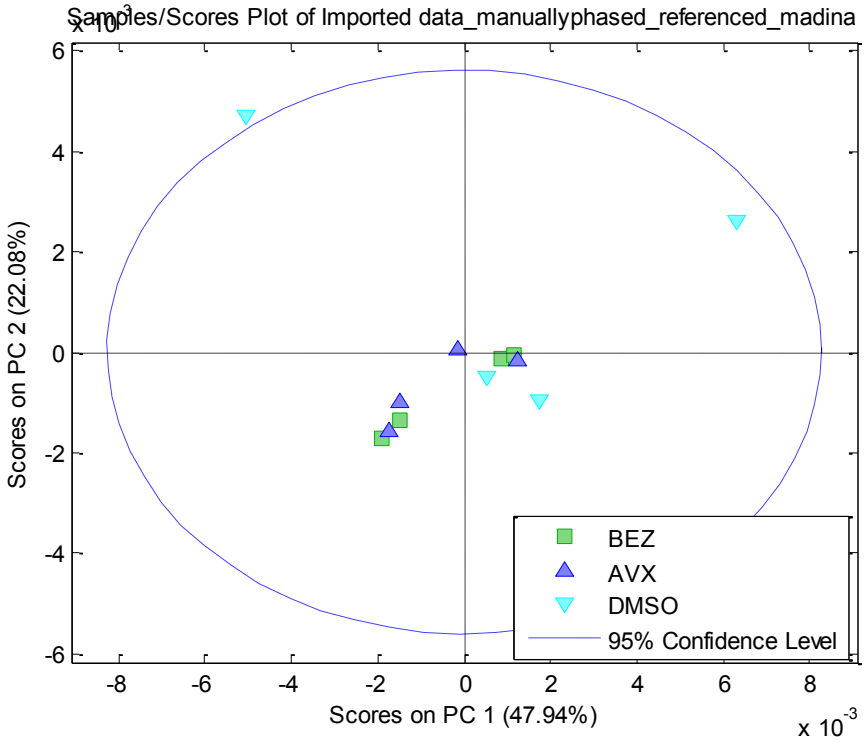

Figure 4.8. Score plot and loading profiles of AVX235, BEZ235 and DMSO from PCA of ^{1}H NMR spectra of cell extracts. Bi-plot based on PC1 and PC2. DMSO1 and DMSO2 are showing abnormal variation.

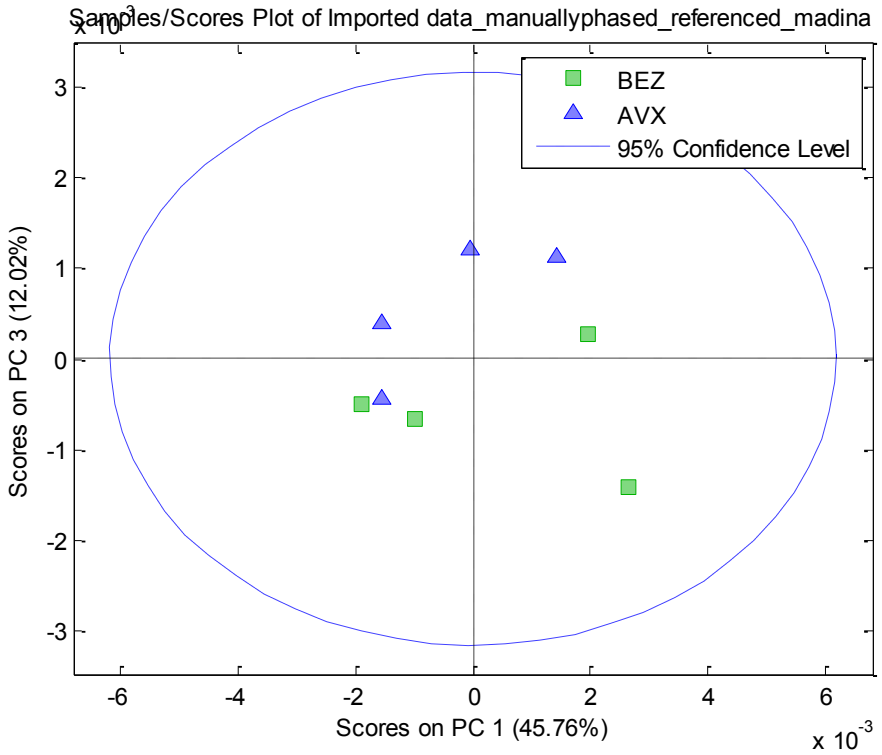

Figure 4.9. Score plot and loading profiles of AVX235 and BEZ235 without control DMSO from PCA of ^{1}H NMR spectra of cell extracts. Bi-plot based on PC1 and PC3.

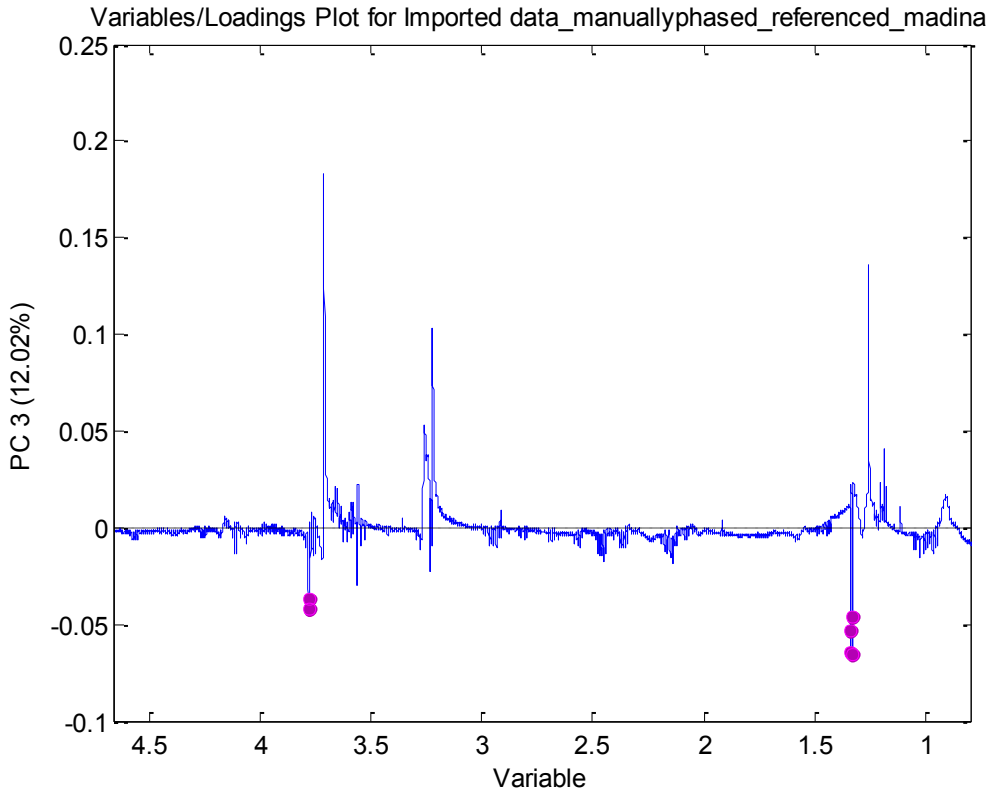

Figure 4.10. PC3 loadings from ^{1}H NMR spectra with differences in lactate peaks shown in purple.

^{1}H NMR spectra provides big amount of information about metabolites. In our results, we observed difference in PCA and separate integration of each peak. Figure 4.10 shows difference between BEZ235 and AVX235 treated groups with more lactate on BEZ235 spectra. However, graph on figure 4.11 shows AVX235 with high lactate. In general, AVX235 demonstrated highest metabolite production compared to BEZ235 treated and DMSO control groups. This difference happened because of disregarding amount of cells during PCA.

Manual spectra alignment of all samples also showed higher PC and GPC peaks in BEZ235 treated group compared to AVX235 treated group (Figure 4.12) with DMSO control group having lowest peaks. Ratio of PC/GPC was calculated considering cell numbers and shows highest results in AVX235 treated group. Altogether PC/GPC ratio is similar in all sample groups without significant difference (Table 4.13).

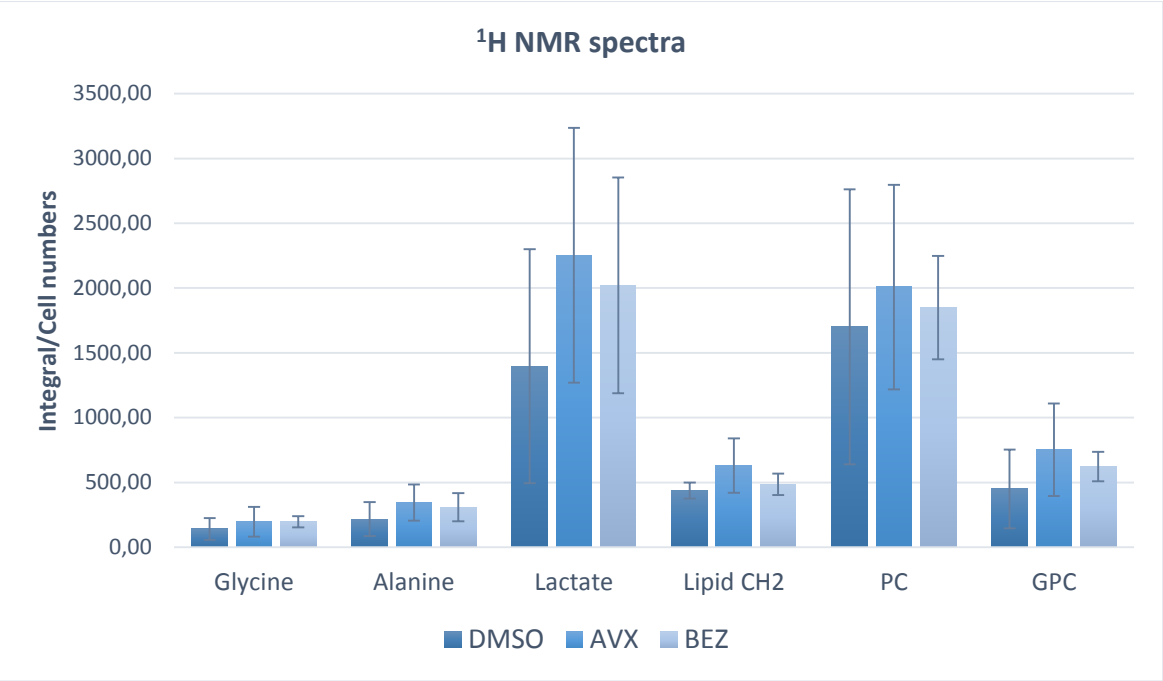

Figure 4.11. Different metabolite levels in MDA-MB-231 breast cancer cells treated with AVX235, BEZ235 and DMSO as a control. Values were quantified from ^{1}H NMR spectra in respect to cell numbers in each sample separately. Standard deviation among sample values is given as error bars.

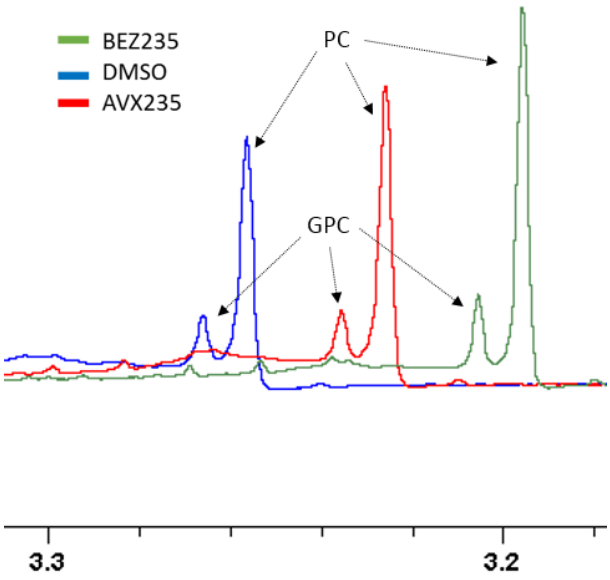

Figure 4.12. Representative ^{1}H NMR spectra of MDA-MB-231 breast cancer cells treated with AVX235 (red), BEZ235 (green) and DMSO as control (blue). All spectra of samples were aligned and zoomed out. To see clear differences in peaks sizes DMSO spectra was shifted left to +0.306

ppm and BEZ235 spectra was shifted right to -0.301 ppm. AVX235 spectra remains on original position with PC peak at 3.22 ppm. PC and GPC peaks are compared.

Table 4.13. Shows ratio between PC and GPC levels quantified from ^{1}H NMR spectra of MDA-MB-231 breast cancer cells treated with AVX235, BEZ235 and DMSO as a control. Standard deviation is given. P value is calculated: AVX235 vs control and BEZ235 vs control.

	DMSO	AVX235	BEZ235
PC/GPC	3,83	2,76	2,98
SD -/+	1,26	0,43	0,48
p-value		0,19	0,28

4.5. ^{13}C NMR spectra

^{13}C NMR spectroscopy was performed to see metabolic flux of glucose in breast cancer cells in response to AVX235 treatment. Derivatives of 1,2-13C labeled glucose are able to observe on spectra. In total 8 samples of ^{13}C NMR spectra were obtained. Due to the curviness of some spectra, it was difficult to align them together at whole range. Instead, most prominent fragments were aligned and compared. There were no glucose peaks on all spectra to report and peaks in general were very weak. Glutamate, lactate, alanine and some contamination peaks were observed and measured. Only glutamate and lactate had strong enough peaks on all samples' spectra to compare them. From spectra analysis it was clear that AVX235 treated samples had highest glutamate peak and BEZ235 treated samples had highest lactate peaks. Integral calculations regarding cell numbers in samples were corresponding to this result. Interestingly, the lactate amount did not correspond in ^{1}H and ^{13}C NMR spectra results. ^{13}C NMR spectra showed higher level of lactate in BEZ235 treated cells while ^{1}H NMR spectra had lactate highest in AVX235 treated cells.

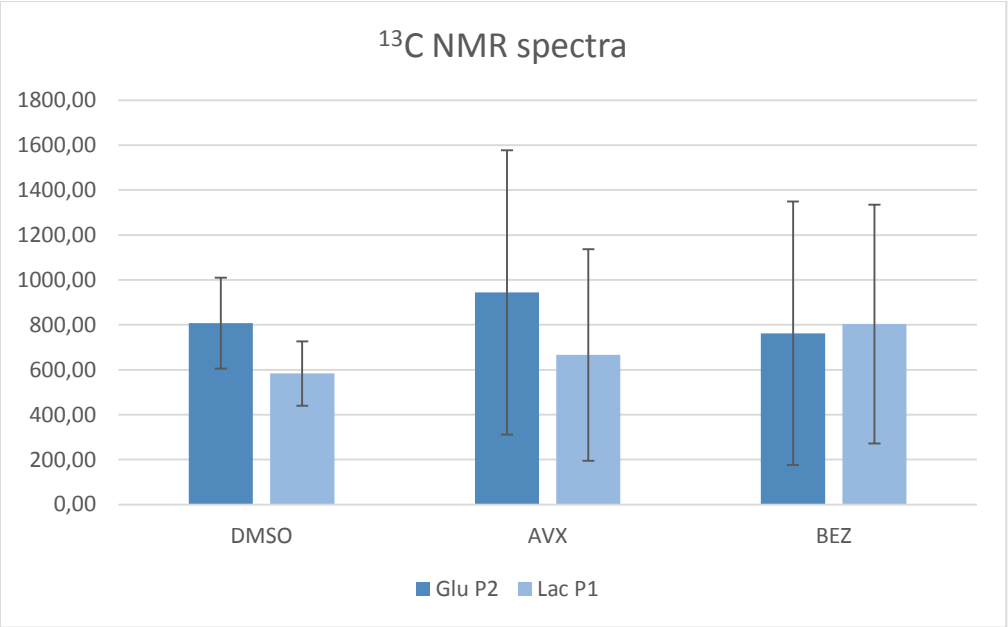

Figure 4.14. Glutamate and lactate levels in MDA-MB-231 breast cancer cells treated with AVX235, BEZ235 and DMSO as control. Values were quanified from ^{13}C NMR spectra in respect to cell numbers in each sample separately. Standard deviation among sample values is given as error bars.

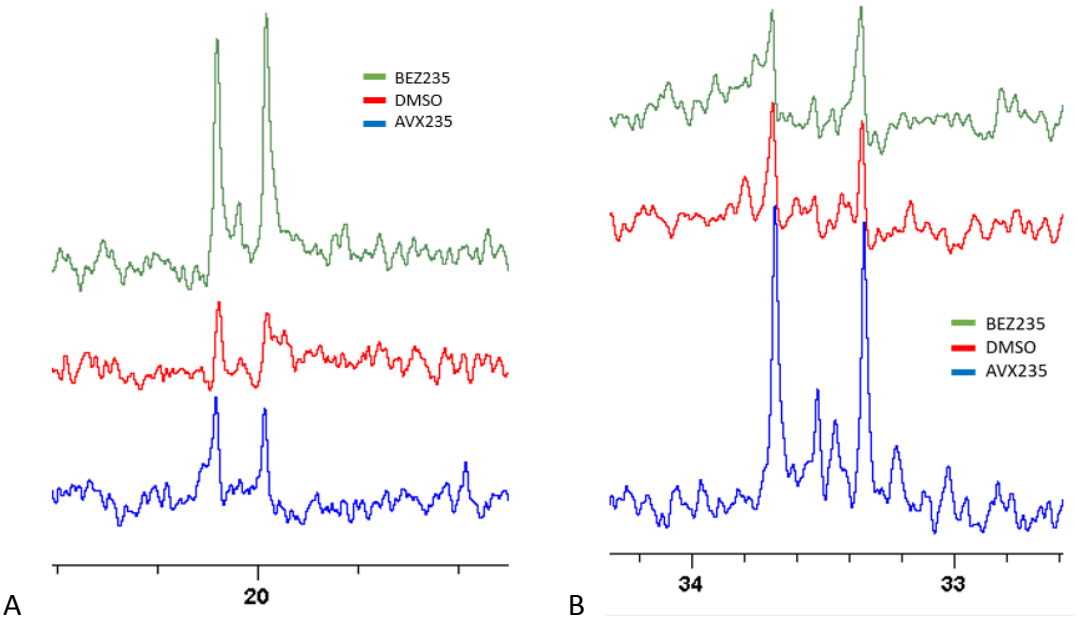

A B

Figure 4.15. Representative ^{13}C NMR spectra of MDA-MB-231 breast cancer cells treated with AVX235 (blue), BEZ235 (green) and DMSO as control (red). All spectra of samples were aligned and zoomed out. To see clear differences in peaks sizes DMSO and BEZ235 spectra were shifted up. AVX235 spectra remains at original position with (A) lactate peak at 20.05 ppm and (B) glutamate peak at 33.5 ppm.

5. DISCUSSION

5.1. Histopathology and mitotic cells counting

The aim of this project was to describe response to the cPLA2 inhibitor AVX235 in basal-like breast cancer, both *in vivo* and *in vitro*. First, tumor slices from an *in vivo* study were evaluated using histopathology. Second, inhibitory effects of AVX235 on breast cancer cells *in vitro* was evaluated. Finally, we used NMR spectrometry to evaluate the metabolic profile of breast cancer cell in response to AVX235 treatment.

Anti-vascularity effect of AVX235 on xenograft mice models was shown in previous study [97]. Slide samples were from this study as well as follow up studies. Purpose of this counting was to see immediate effect of AVX235 on proliferation rate of tumor cells and therefore slides of second and fifth days were counted.

We used two different immunohistochemical markers to observe proliferative activity in tumor samples: PHH3 and anti-ki67/Lectin stainings. From microscope observation of stained sample slides, there were observable differences between these two different markers for proliferation. With PHH3, it was easier to identify and count mitotic cells. However, there were no significant differences in mitotic cell numbers between treated and control cell samples. Slides were stained with different staining to have stronger evidence on proliferation. If both staining showed no significantly difference, then our results would be more reliable.

Anti-ki67/lectin staining displayed some parts of background of cells or extracellular matrix (ECM) by staining carbohydrates in endothelial cells into blue with lectin. Anti-ki67 binds to ki67 protein involved in proliferation and located in nucleus region, which stains it to brown. This technique highlights proliferating cells, but in our case, it was harder to identify them. In PHH3 staining histone proteins are stained in brown and in our samples nucleuses of mitotic cells were clearer and easier to identify in comparison to anti-ki67/lectin staining. There were no significant differences in proliferative cell numbers between all control and treated groups. In addition, ratio of mitotic cells in each day group between control and treated samples were similar in both staining. Samples of two stainings showed various results in difference between second and fifth days of treatment. Ki67/lectin slides showed no significant change in proliferative cell numbers at fifth day's slides in both control and treated. Whereas PHH3 stained samples, had decrease in proliferative cell numbers at fifth day's slides in both control and treated. These results showed

significant *p*-value, but not between control and treated. This decrease of proliferative cells on fifth day may happen because of various reasons regarding whole organism of these particular animal and tumor progression in general.

Samples used in this thesis were from HR MAS cohort of Kim et al group's previous study on anti-vascular effect of AVX235 in tumor where they used automated image reading system of custom MATLAB to count proliferative cells [97]. They did not observe any significant difference of cell proliferation between control and treated groups at an early time point. Nevertheless, they observed decrease in PGE levels, vessel density, vessel maturity and number of proliferating cells in later days of treatment. However, PGE2 levels were significantly lower on second day of AVX235 treatment, but it was not reflected in cell proliferation rate. PGE2 is downstream metabolite of cPLA2 which was reported in breast cancer and other cancer types too [122]. As the group suggested this may also be due to the relatively small group sizes in their study or simply some errors in histological analysis.

In general, counting cells under microscope in person is subjective; different pathologists may have slightly different results and this may be significant in some cases. Here, I counted all cells alone and compared results with those of a professional pathologist who controlled them. In addition to that, I counted cells in blind, without knowing which slides were from control and treated groups, as they were all coded with numbers and I recorded my results according to these codes. My results show that cPLA2IVA inhibition with AVX235 may not affect proliferation rate in early days of treatment of MAS98.12 mice. However, as it was shown in previous study, the effect may come on later points of treatment. In addition, effect may be not directly in proliferation but instead in metabolic profile of cancer cells and long-term tumor by modulating vascular features.

5.2. Cell growth curve

Although we observed effect of AVX235 *in vivo* in previous study, it is also necessary to elucidate molecular pathways of different metabolites on cellular level. Inhibition of cPLA2 has been shown to decrease growth in many types of cancer cells [123]. It was important to see if AVX235 has an effect on growth or proliferation.

Cell growth experiments were performed for training purpose and to establish growth rate of MDA-MB-231 cell line. This experiment helped me to get used to work with breast cancer cells and learn how to maintain them. Procedure was made according to providers (ATCC) recommendations with slight modifications and results were compared thereafter with theirs [121]. Since MDA-MB-231 cell line were originally established from tumor in basal cells they have interesting morphology which can change as response to stress of new passage. This was observed during experiments. Cells in new passage were star like shaped with stretched spindles to reach other neighboring cells and in high confluency, they had round polygonal shape. In our cell growth curve we got similar results with ATCC (Figure 3.3). We observed cell growth six days while ATCC had eight days results. After fifth days ATCC cell growth showed stationary phase of no significant increase in numbers most probably due to the total cover of flask surface. We used T25 flasks and had no stationary phase, despite almost 100% confluency. Usually after stationary phase comes decline phase when proliferation rate drops down, but MDA-MB-231 cell line is one of aggressive cancer lines and it forms multilayer and would not stop proliferating unless it starved [124]. Our growth curve showed exponential increase of cells number in log phase with doubling period 30 hours in comparison of ATCC's 38 hours. This difference may be because of different serum type or growth medium, ATCC used L-15 and we used DMEM. Also ATCC performed cell counting with automated counter and I counted using a Bürker chamber.

5.3. MTT viability assay

In order to investigate the toxicity of AVX235 in MDA-MB-231, MCF-7 and SK-BR-3 breast cancer cell lines, MTT viability assay was performed. From the data of previous studies of different breast cancer cell lines, it was established high expression of cPLA2 in breast cancer cells with malignancy and high aggressiveness [125]. In the report of Caiazza et al, cPLA2 levels in different breast cancer cell lines were measures and compared. MDA-MB-231 cells showed highest level and mRNA expression of cPLA2 with MCF-7 cells as lowest [126]. Due to this, we would expect lowest viability in MDA-MB-231 cells, in response to cPLA2 inhibition, however we got different result. IC50 graphs of all cell lines look similar and had relatively similar values: MDA-MB-231 - 29.7 µM, MCF-7 - 27.1 µM and SK-BR-3 - 23.6 µM concentration of AVX235.

Only one of three MTT experiments was successful, as there were some technical errors and due to this, results are not reported. Hence, the results reported are statistically weak it is hard to

make assumptions on them, though one successful assay was in line with other lab members' result.

5.4. NMR spectra analysis

In order to examine metabolic profile of breast cancer cell in response to AVX235 treatment we used NMR spectrometry. We could see trend of increase in PC and GPC levels in response to inhibition of cPLA2 in MDA-MB-231 cells with AVX235 compared to BEZ235 (PI3K inhibitor) treated group and DMSO control group. Other metabolites such as lactate, alanine, glycine and some CH2 lipids were also elevated in treated groups compared to control. Choline is actively transported into cells through various organic cation transporters and it was reported that MDA-MB-231 cells do not have overexpression of these transporters, though choline transport rate was high, which concludes in active transport of choline [39, 127]. Further, this intracellular choline metabolized through Kennedy pathway (Figure 1.2). Many studies associate high choline components level with invasiveness, it was demonstrated that when metastasis suppressor genes nm23 were transfected to malignant breast cancer cells, they exhibited significantly lower ratio of PC/GPC [128]. In another study of same group of Aboagye et al, they report increase of PC and decrease of GPC levels in response to under expression of cPLA2IVA group [129, 130], which is corresponding to our results. Inhibition of cPLA2 with AVX235 could cause increase of PC and decrease of GPC levels compared to DMSO control group, since cPLA2 activity generates lysoPtdCho, which is then hydrolyzed to free fatty acids and GPC, in addition PtdCho is hydrolyzed to PC and diacylglycerol [131]. Inhibition of PI3K pathway with BEZ235 treatment is also show increase of PC and GPC levels, not as high as with AVX235 treatment. However, statistical calculation t-test did not show significant difference between AVX235 vs control and AVX235 vs BEZ235 treatment groups in metabolite product amounts. This may be because of small amount of samples we analyzed.

Phospatidylcholine (PtdCho) as a product of the choline pathway (Figure 1.2) is the main phospholipid composing cellular membrane. When AVX235 inhibits cPLA2 it increase PtdCho level. It is not possible to detect PtdCho in ^{13}C and ^{1}H NMR spectra. Accumulated PtdCho also should take role in elevation of choline and PC levels. Further intracellular choline is phosphorylated into PC by the enzyme choline kinase (ChoK) again, which is working actively in

MDA-MB-231 breast cancer cells [39] and this might be reason of absence of choline peak on spectra.

Since our ^{13}C NMR spectra had very weak peaks of all metabolites, it was hard to observe glucose metabolic pathway. There were no glucose peaks on spectra. This may be because of total consumption of 1,2-13C labeled glucose, which is very unlikely, or due to some technical error during experiment regarding glucose concertation. Nevertheless, we could observe some peaks of lactate and glutamate on all spectra and were able to measure it to compare samples (Figure 3.16). Lactate is product of aerobic glycolysis in cancer cells and glutamate is product of TCA cycle (Figure 1.8). ^{13}C NMR spectra results showed highest level of glutamate in AVX235 treated group. High level of glutamate in breast cancer cells were reported before in regards of malignancy and invasiveness [132, 133]. BEZ235 treated samples had highest lactate amount in ^{13}C NMR spectra, which is contradicting with our ^{1}H NMR spectra results where lactate was highest in AVX235, treated group. This may be due to the additional amount of lactate produced not from labeled glucose, but from glucose in media. However, all calculated amounts of produced metabolites showed insignificant result on t-test with p-value > 0.5.

Inhibition of PI3K pathway with BEZ235 treatment of basal like xenografts showed reduction of lactate concentration in previous studies [134], while we had another interesting results in levels of lactate in ^{1}H NMR spectra. High lactate level is sign of invasiveness in cancer cells, due to the lactate property of acidification of extracellular environment, which promotes cells detachment from extracellular matrix [135]. Since lactate transport out of cell is not clear, intracellular and extracellular lactate is measured as one [136], that also can be reason of our spectra result differences. Results evaluated with consideration of cell numbers in each sample showed higher level in AVX235 treated group (Figure 4.11) when PCA of all spectra without considering cell numbers showed higher lactate level in BEZ235 treated group (Figure 4.12). Considering cell amount showed difference in rank distribution of metabolites with AVX235 treated group showing highest production of all of them, although statistical testing did not show significant difference there either. Results with considering cell numbers supposed to give reliable values, since it would be per cell production.

6. CONCLUSION AND FUTURE PERSPECTIVES

By evaluating all gathered results from our experiments and reports from previous research, it is hard to make a solid conclusion.

From MTT assay, we can see viability of MDA-MB-231 cells in response to inhibition of cPLA2 by different concentrations of AVX235. AVX235 over 30 µM concentration effects cell growth dramatically, it inhibits proliferation of cells. However, in 10 µM we did not observe inhibition of proliferation in MDA-MB-231 cells, which is supported by metabolic activity from ^{1}H NMR spectra results too. Effect of cPLA2 inhibition in breast cancer cells with AVX235 needs more research, since there are not so many published articles on this subject yet.

For future studies, I would recommend to increase AVX235 concentration around 20 µM to see proliferative inhibition in cells and prolong treatment period. It would be efficient to measure cPLA2 expression and activity in parallel.

7. REFERENCE

1. Jemal, A., et al., *Global cancer statistics.* CA Cancer J Clin, 2011. **61**(2): p. 69-90.
2. WHO. *World Cancer Report 2014*. WHO Press [Report] 2015 February 2015; Available from: http://www.iarc.fr/en/publications/books/wcr/wcr-order.php.
3. Lodish H, B.A., Zipursky SL, et al., *Proto-Oncogenes and Tumor-Suppressor Genes.*, in *Molecular Cell Biology.*, N.Y.W.H. Freeman, Editor. 2000.
4. Hanahan, D. and R.A. Weinberg, *The hallmarks of cancer.* Cell, 2000. **100**(1): p. 57-70.
5. Hanahan, D. and R.A. Weinberg, *Hallmarks of Cancer: The Next Generation.* Cell, 2011. **144**(5): p. 646-674.
6. DeVita , V.T.J. and S.A. Rosenberg *Two Hundred Years of Cancer Research.* New England Journal of Medicine, 2012. **366**(23): p. 2207-2214.
7. Tímár, J., et al., *Genetic progression of malignant melanoma.* Cancer and Metastasis Reviews, 2016. **35**(1): p. 93-107.
8. Peto, R., et al., *UK and USA breast cancer deaths down 25% in year 2000 at ages 20–69 years.* The Lancet, 2000. **355**(9217): p. 1822.
9. WHO. *The Global Burden of Disease: Geneva*. 2008; World Health Organization].
10. Cardiff, R.D. and A.D. Borowsky, *At last: classification of human mammary cells elucidates breast cancer origins.* The Journal of Clinical Investigation, 2014. **124**(2): p. 478-480.
11. Veronesi, U., et al., *Breast cancer.* Lancet, 2005. **365**(9472): p. 1727-41.
12. Yoshida, K. and Y. Miki, *Role of BRCA1 and BRCA2 as regulators of DNA repair, transcription, and cell cycle in response to DNA damage.* Cancer Sci, 2004. **95**(11): p. 866-71.
13. Venkitaraman, A.R., *Functions of BRCA1 and BRCA2 in the biological response to DNA damage.* Journal of Cell Science, 2001. **114**(20): p. 3591-3598.
14. Weigelt, B. and J.S. Reis-Filho, *Histological and molecular types of breast cancer: is there a unifying taxonomy?* Nat Rev Clin Oncol, 2009. **6**(12): p. 718-30.
15. Weigelt, B., F.C. Geyer, and J.S. Reis-Filho, *Histological types of breast cancer: How special are they?* Molecular Oncology, 2010. **4**(3): p. 192-208.
16. Hallett, R.M., et al., *Identification and evaluation of network modules for the prognosis of basal-like breast cancer.* Oncotarget, 2015. **6**(19): p. 17713-24.
17. Prat, A., et al., *Phenotypic and molecular characterization of the claudin-low intrinsic subtype of breast cancer.* Breast Cancer Research, 2010. **12**(5): p. 1-18.
18. Sabatier, R., et al., *Claudin-low breast cancers: clinical, pathological, molecular and prognostic characterization.* Molecular Cancer, 2014. **13**(1): p. 1-14.
19. Perou, C.M., et al., *Molecular portraits of human breast tumours.* Nature, 2000. **406**(6797): p. 747-752.
20. Singletary, S.E. and J.L. Connolly, *Breast Cancer Staging: Working With the Sixth Edition of the AJCC Cancer Staging Manual.* CA: A Cancer Journal for Clinicians, 2006. **56**(1): p. 37-47.
21. Yu, K.-D., S. Li, and Z.-M. Shao, *Different Annual Recurrence Pattern Between Lumpectomy and Mastectomy: Implication for Breast Cancer Surveillance After Breast-Conserving Surgery.* The Oncologist, 2011. **16**(8): p. 1101-1110.
22. Puhalla, S., S. Bhattacharya, and N.E. Davidson, *Hormonal therapy in breast cancer: A model disease for the personalization of cancer care.* Molecular Oncology, 2012. **6**(2): p. 222-236.
23. Chavez-MacGregor, M., et al., *DElayed initiation of adjuvant chemotherapy among patients with breast cancer.* JAMA Oncology, 2016. **2**(3): p. 322-329.
24. Hoefnagel, L.D., et al., *Receptor conversion in distant breast cancer metastases.* Breast Cancer Research, 2010. **12**(5): p. 1-9.
25. Rakha, E.A., J.S. Reis-Filho, and I.O. Ellis, *Basal-like breast cancer: a critical review.* J Clin Oncol, 2008. **26**(15): p. 2568-81.
26. Sorlie, T., et al., *Gene expression patterns of breast carcinomas distinguish tumor subclasses with clinical implications.* Proc Natl Acad Sci U S A, 2001. **98**(19): p. 10869-74.

27. Minami, C.A., D.U. Chung, and H.R. Chang, *Management Options in Triple-Negative Breast Cancer.* Breast Cancer : Basic and Clinical Research, 2011. **5**: p. 175-199.
28. Prat, A., et al., *Predicting response and survival in chemotherapy-treated triple-negative breast cancer.* Br J Cancer, 2014. **111**(8): p. 1532-41.
29. Ou, J., et al., *Prevalence of BRCA1 and BRCA2 Germline Mutations in Breast Cancer Women of Multiple Ethnic Region in Northwest China.* J Breast Cancer, 2013. **16**(1): p. 50-4.
30. Lehmann, B.D., et al., *Identification of human triple-negative breast cancer subtypes and preclinical models for selection of targeted therapies.* J Clin Invest, 2011. **121**(7): p. 2750-67.
31. Carey, L., et al., *Triple-negative breast cancer: disease entity or title of convenience?* Nat Rev Clin Oncol, 2010. **7**(12): p. 683-692.
32. Lopez-Knowles, E., et al., *PI3K pathway activation in breast cancer is associated with the basal-like phenotype and cancer-specific mortality.* Int J Cancer, 2010. **126**(5): p. 1121-31.
33. Moulder, S.L., *Does the PI3K pathway play a role in basal breast cancer?* Clin Breast Cancer, 2010. **10 Suppl 3**: p. S66-71.
34. Maira, S.M., et al., *Identification and characterization of NVP-BEZ235, a new orally available dual phosphatidylinositol 3-kinase/mammalian target of rapamycin inhibitor with potent in vivo antitumor activity.* Mol Cancer Ther, 2008. **7**(7): p. 1851-63.
35. Dang, C.V., *Links between metabolism and cancer.* Genes & Development, 2012. **26**(9): p. 877-890.
36. Seyfried, T.N. and L.M. Shelton, *Cancer as a metabolic disease.* Nutrition & Metabolism, 2010. **7**(1): p. 1-22.
37. Annibaldi, A. and C. Widmann, *Glucose metabolism in cancer cells.* Curr Opin Clin Nutr Metab Care, 2010. **13**(4): p. 466-70.
38. Cairns, R.A., I.S. Harris, and T.W. Mak, *Regulation of cancer cell metabolism.* Nat Rev Cancer, 2011. **11**(2): p. 85-95.
39. Eliyahu, G., T. Kreizman, and H. Degani, *Phosphocholine as a biomarker of breast cancer: Molecular and biochemical studies.* International Journal of Cancer, 2007. **120**(8): p. 1721-1730.
40. Bolan, P.J., et al., *In vivo quantification of choline compounds in the breast with 1H MR spectroscopy.* Magnetic Resonance in Medicine, 2003. **50**(6): p. 1134-1143.
41. Glunde, K., Z.M. Bhujwalla, and S.M. Ronen, *Choline metabolism in malignant transformation.* Nat Rev Cancer, 2011. **11**(12): p. 835-48.
42. Glunde, K., M.A. Jacobs, and Z.M. Bhujwalla, *Choline metabolism in cancer: implications for diagnosis and therapy.* Expert Rev Mol Diagn, 2006. **6**(6): p. 821-9.
43. Caiazza, F., et al., *Cytosolic phospholipase A2-alpha expression in breast cancer is associated with EGFR expression and correlates with an adverse prognosis in luminal tumours.* Br J Cancer, 2011. **104**(2): p. 338-44.
44. Moestue, S., et al., *HR MAS MR spectroscopy in metabolic characterization of cancer.* Curr Top Med Chem, 2011. **11**(1): p. 2-26.
45. Mader, C., *The Biology of Cancer.* The Yale Journal of Biology and Medicine, 2007. **80**(2): p. 91-91.
46. Weinberg, R.A., *The Biology of cancer*. Second ed. 2014: Garland Sience, Taylor & Francis.
47. Warburg, O., F. Wind, and E. Negelein, *Über den Stoffwechsel von Tumoren im Körper.* Klinische Wochenschrift, 1926. **5**(19): p. 829-832.
48. Marie, S.K.N. and S.M.O. Shinjo, *Metabolism and Brain Cancer.* Clinics, 2011. **66**(Suppl 1): p. 33-43.
49. Wigerup, C., S. Pahlman, and D. Bexell, *Review: Therapeutic targeting of hypoxia and hypoxia-inducible factors in cancer.* Pharmacol Ther, 2016.
50. Ke, Q. and M. Costa, *Hypoxia-inducible factor-1 (HIF-1).* Mol Pharmacol, 2006. **70**(5): p. 1469-80.
51. Warburg, O., *On the origin of cancer cells.* Science, 1956. **123**(3191): p. 309-14.
52. Macheda, M.L., S. Rogers, and J.D. Best, *Molecular and cellular regulation of glucose transporter (GLUT) proteins in cancer.* J Cell Physiol, 2005. **202**(3): p. 654-62.
53. Vander Heiden, M.G., L.C. Cantley, and C.B. Thompson, *Understanding the Warburg Effect: The Metabolic Requirements of Cell Proliferation.* Science (New York, N.Y.), 2009. **324**(5930): p. 1029-1033.

54. Martinez-Zaguilan, R., et al., *Acidic pH enhances the invasive behavior of human melanoma cells.* Clin Exp Metastasis, 1996. **14**(2): p. 176-86.
55. Rozhin, J., et al., *Pericellular pH affects distribution and secretion of cathepsin B in malignant cells.* Cancer Res, 1994. **54**(24): p. 6517-25.
56. Gottschalk, S., et al., *Imatinib (STI571)-mediated changes in glucose metabolism in human leukemia BCR-ABL-positive cells.* Clin Cancer Res, 2004. **10**(19): p. 6661-8.
57. Polyak, K., *Heterogeneity in breast cancer.* The Journal of Clinical Investigation, 2011. **121**(10): p. 3786-3788.
58. Lacroix, M. and G. Leclercq, *Relevance of breast cancer cell lines as models for breast tumours: an update.* Breast Cancer Res Treat, 2004. **83**(3): p. 249-89.
59. Cespedes, M.V., et al., *Mouse models in oncogenesis and cancer therapy.* Clin Transl Oncol, 2006. **8**(5): p. 318-29.
60. Kerbel, R.S., *Human tumor xenografts as predictive preclinical models for anticancer drug activity in humans: better than commonly perceived-but they can be improved.* Cancer Biol Ther, 2003. **2**(4 Suppl 1): p. S134-9.
61. Eklund, L., M. Bry, and K. Alitalo, *Mouse models for studying angiogenesis and lymphangiogenesis in cancer.* Mol Oncol, 2013. **7**(2): p. 259-82.
62. Marangoni, E., et al., *A new model of patient tumor-derived breast cancer xenografts for preclinical assays.* Clin Cancer Res, 2007. **13**(13): p. 3989-98.
63. Workman, P., et al., *Guidelines for the welfare and use of animals in cancer research.* Br J Cancer, 2010. **102**(11): p. 1555-77.
64. Bertucci, F. and D. Birnbaum, *Reasons for breast cancer heterogeneity.* Journal of Biology, 2008. **7**(2): p. 6-6.
65. Burke, J.E. and E.A. Dennis, *Phospholipase A(2) structure/function, mechanism, and signaling.* Journal of Lipid Research, 2009. **50**(Suppl): p. S237-S242.
66. Vines, C.M. and C.A. Bill, *Phospholipases*, in *eLS*. 2001, John Wiley & Sons, Ltd.
67. Chap, H., *Forty five years with membrane phospholipids, phospholipases and lipid mediators: A historical perspective.* Biochimie, 2016. **125**: p. 234-249.
68. Yashad Dongol, B.L.D., Rakesh Kumar Shrestha and Gopi Aryal, *Pharmacological and Immunological Properties of Wasp Venom*. Pharmacological and Immunological Properties of Wasp Venom. 2014: CC BY 3.0 license The Author(s).
69. Brown, H.A. and L.J. Marnett, *Introduction to Lipid Biochemistry, Metabolism, and Signaling.* Chemical Reviews, 2011. **111**(10): p. 5817-5820.
70. Shimuta, K., et al., *The hemolytic and cytolytic activities of Serratia marcescens phospholipase A (PhlA) depend on lysophospholipid production by PhlA.* BMC Microbiol, 2009. **9**: p. 261.
71. Imae, R., et al., *Intracellular phospholipase A1 and acyltransferase, which are involved in Caenorhabditis elegans stem cell divisions, determine the sn-1 fatty acyl chain of phosphatidylinositol.* Mol Biol Cell, 2010. **21**(18): p. 3114-24.
72. Richmond, G.S. and T.K. Smith, *Phospholipases A(1).* International Journal of Molecular Sciences, 2011. **12**(1): p. 588-612.
73. Franson, R., M. Waite, and M. LaVia, *Identification of phospholipase A 1 and A 2 in the soluble fraction of rat liver lysosomes.* Biochemistry, 1971. **10**(10): p. 1942-6.
74. Sommerfelt, R.M., et al., *Cytosolic phospholipase A2 modulates TLR2 signaling in synoviocytes.* PLoS One, 2015. **10**(4): p. e0119088.
75. Dennis, E.A., et al., *Phospholipase A(2) Enzymes: Physical Structure, Biological Function, Disease Implication, Chemical Inhibition, and Therapeutic Intervention.* Chemical reviews, 2011. **111**(10): p. 6130-6185.
76. Chakraborti, S., *Phospholipase A(2) isoforms: a perspective.* Cell Signal, 2003. **15**(7): p. 637-65.
77. Murakami, M., et al., *Recent progress in phospholipase A2 research: From cells to animals to humans.* Progress in Lipid Research, 2011. **50**(2): p. 152-192.
78. Glaser, K.B., *Regulation of phospholipase A2 enzymes: selective inhibitors and their pharmacological potential.* Adv Pharmacol, 1995. **32**: p. 31-66.

79. Dulin, N.O., et al., *Phospholipase A(2)-mediated activation of mitogen-activated protein kinase by angiotensin II.* Proceedings of the National Academy of Sciences of the United States of America, 1998. **95**(14): p. 8098-8102.
80. Stephenson, D.T., et al., *Calcium-sensitive cytosolic phospholipase A2 (cPLA2) is expressed in human brain astrocytes.* Brain Res, 1994. **637**(1-2): p. 97-105.
81. Tjandrawinata, R.R., R. Dahiya, and M. Hughes-Fulford, *Induction of cyclo-oxygenase-2 mRNA by prostaglandin E2 in human prostatic carcinoma cells.* Br J Cancer, 1997. **75**(8): p. 1111-8.
82. Wang, D. and R.N. DuBois, *Eicosanoids and cancer.* Nat Rev Cancer, 2010. **10**(3): p. 181-193.
83. Wen, Z.H., et al., *Critical role of arachidonic acid-activated mTOR signaling in breast carcinogenesis and angiogenesis.* Oncogene, 2013. **32**(2): p. 160-70.
84. Nakanishi, M. and D.W. Rosenberg, *Roles of cPLA2alpha and arachidonic acid in cancer.* Biochim Biophys Acta, 2006. **1761**(11): p. 1335-43.
85. Nakanishi, M. and D.W. Rosenberg, *Multifaceted roles of PGE(2) in inflammation and cancer().* Seminars in immunopathology, 2013. **35**(2): p. 123-137.
86. Park, J.Y., M.H. Pillinger, and S.B. Abramson, *Prostaglandin E2 synthesis and secretion: The role of PGE2 synthases.* Clinical Immunology, 2006. **119**(3): p. 229-240.
87. Sommerfelt, R.M., *Molecular mechanisms of inflammation – a central role for cytosolic phospholipase A2*, in *Fakultet for naturvitenskap og teknologi, Institutt for biologi*. 2014, Norges teknisk-naturvitenskapelige universitet.
88. Hurley, B.P., N.L. Williams, and B.A. McCormick, *Involvement of phospholipase A2 in Pseudomonas aeruginosa-mediated PMN transepithelial migration.* Am J Physiol Lung Cell Mol Physiol, 2006. **290**(4): p. L703-l709.
89. Linkous, A. and E. Yazlovitskaya, *Cytosolic phospholipase A2 as a mediator of disease pathogenesis.* Cellular Microbiology, 2010. **12**(10): p. 1369-1377.
90. Yu, Y., et al., *Epidermal growth factor induces platelet-activating factor production through receptors transactivation and cytosolic phospholipase A(2) in ovarian cancer cells.* Journal of Ovarian Research, 2014. **7**: p. 39-39.
91. Thotala, D., et al., *Cytosolic phospholipaseA2 inhibition with PLA-695 radiosensitizes tumors in lung cancer animal models.* PLoS One, 2013. **8**(7): p. e69688.
92. Yazlovitskaya, E.M., et al., *Cytosolic phospholipase A2 regulates viability of irradiated vascular endothelium.* Cell Death Differ, 2008. **15**(10): p. 1641-53.
93. Linkous, A., et al., *Cytosolic phospholipase A2: targeting cancer through the tumor vasculature.* Clin Cancer Res, 2009. **15**(5): p. 1635-44.
94. Linkous, A.G., E.M. Yazlovitskaya, and D.E. Hallahan, *Cytosolic Phospholipase A2 and Lysophospholipids in Tumor Angiogenesis.* JNCI Journal of the National Cancer Institute, 2010. **102**(18): p. 1398-1412.
95. Singh-Ranger, G., M. Salhab, and K. Mokbel, *The role of cyclooxygenase-2 in breast cancer: review.* Breast Cancer Research and Treatment, 2008. **109**(2): p. 189-198.
96. Kokotos, G., et al., *Inhibition of group IVA cytosolic phospholipase A2 by thiazolyl ketones in vitro, ex vivo, and in vivo.* J Med Chem, 2014. **57**(18): p. 7523-35.
97. Kim, E., et al., *Anti-vascular effects of the cytosolic phospholipase A2 inhibitor AVX235 in a patient-derived basal-like breast cancer model.* BMC Cancer, 2016. **16**(1): p. 191.
98. Rabi, I.I., et al., *A New Method of Measuring Nuclear Magnetic Moment.* Physical Review, 1938. **53**(4): p. 318-318.
99. Bloch, F., W.W. Hansen, and M. Packard, *The Nuclear Induction Experiment.* Physical Review, 1946. **70**(7-8): p. 474-485.
100. Purcell, E.M., H.C. Torrey, and R.V. Pound, *Resonance Absorption by Nuclear Magnetic Moments in a Solid.* Physical Review, 1946. **69**(1-2): p. 37-38.
101. Smith-Bindman, R., et al., *Use of diagnostic imaging studies and associated radiation exposure for patients enrolled in large integrated health care systems, 1996-2010.* Jama, 2012. **307**(22): p. 2400-9.
102. Fass, L., *Imaging and cancer: a review.* Mol Oncol, 2008. **2**(2): p. 115-52.

103. Ala-Korpela, M., *Critical evaluation of 1H NMR metabonomics of serum as a methodology for disease risk assessment and diagnostics.* Clin Chem Lab Med, 2008. **46**(1): p. 27-42.
104. Gillies, R.J. and D.L. Morse, *In vivo magnetic resonance spectroscopy in cancer.* Annu Rev Biomed Eng, 2005. **7**: p. 287-326.
105. Katz-Brull, R., et al., *Metabolic markers of breast cancer: enhanced choline metabolism and reduced choline-ether-phospholipid synthesis.* Cancer Res, 2002. **62**(7): p. 1966-70.
106. Farshidfar, F., et al., *Serum metabolomic profile as a means to distinguish stage of colorectal cancer.* Genome Med, 2012. **4**(5): p. 42.
107. Gobl, C., et al., *NMR approaches for structural analysis of multidomain proteins and complexes in solution.* Prog Nucl Magn Reson Spectrosc, 2014. **80**: p. 26-63.
108. Friebolin, H., *Basic One and Two Dimensional NMR Spectroscopy*. 5 ed. 2011: Weinheim: Wiley-VCH-Verl.
109. Jacobsen, N.E., *NMR Relaxation—Inversion-Recovery and the Nuclear Overhauser Effect (NOE)*, in *NMR Spectroscopy Explained*. 2007, John Wiley & Sons, Inc. p. 155-199.
110. Palmnas, M. and H. Vogel, *The Future of NMR Metabolomics in Cancer Therapy: Towards Personalizing Treatment and Developing Targeted Drugs?* Metabolites, 2013. **3**(2): p. 373.
111. Eakin, R.T. and L.O. Morgan, *Carbon-13 nuclear-magnetic-resonance spectroscopy of whole cells and of cytochrome C from Neurospora crass grown with (S-Me-13C)methionine.* Biochemical Journal, 1975. **152**(3): p. 529-535.
112. Grinde, M.T., et al., *Interplay of choline metabolites and genes in patient-derived breast cancer xenografts.* Breast Cancer Res, 2014. **16**(1): p. R5.
113. Garwood, M., et al., *Magnetic resonance imaging with adiabatic pulses using a single surface coil for RF transmission and signal detection.* Magn Reson Med, 1989. **9**(1): p. 25-34.
114. Buckle, T., et al., *Metabolic reprogramming supports the invasive phenotype in malignant melanoma.* Nat Med, 2015. **366**(1): p. 71-83.
115. Gorad, S.S., *The impact of oncogenic signaling on the metabolomics of melanoma and prostate cancer*, in *Department of Circulation and Medical Imaging*. 2016, NTNU: Faculty of medicine.
116. Ross, B.D., et al., *31P NMR spectroscopy of the in vivo metabolism of an intracerebral glioma in the rat.* Magn Reson Med, 1988. **6**(4): p. 403-17.
117. Ross, B.D., et al., *Carbohydrate metabolism of the rat C6 glioma. An in vivo 13C and in vitro 1H magnetic resonance spectroscopy study.* NMR Biomed, 1988. **1**(1): p. 20-6.
118. Nagana Gowda, G.A., et al., *Metabolomics-Based Methods for Early Disease Diagnostics: A Review.* Expert review of molecular diagnostics, 2008. **8**(5): p. 617-633.
119. Silva Elipe, M.V., *Advantages and disadvantages of nuclear magnetic resonance spectroscopy as a hyphenated technique.* Analytica Chimica Acta, 2003. **497**(1–2): p. 1-25.
120. Ivers, L.P., et al., *Dynamic and influential interaction of cancer cells with normal epithelial cells in 3D culture.* Cancer Cell International, 2014. **14**(1): p. 1-16.
121. (ATCC), A.T.C.C., *Thawing, Propagating and Cryopreserving Protocol NCI-PBCF-HTB26 (MDA-MB-231) Breast Adenocarcinoma*. March 2012, Physical Sciences-Oncology Center Network Bioresource Core facility (PBCF).
122. Greenhough, A., et al., *The COX-2/PGE2 pathway: key roles in the hallmarks of cancer and adaptation to the tumour microenvironment.* Carcinogenesis, 2009. **30**(3): p. 377-86.
123. Tunset, H.M., et al., *cPLA2IVA Inhibition in Basal-Like Breast Cancer: Reduced Tumor Growth with Metabolic, Vascular and Gene Expression Changes*, in *ISMRM 23rd Annual Meeting and Exhibition*. 2015: Toronto.
124. Ye, Q., S. Kantonen, and J. Gomez-Cambronero, *Serum deprivation confers the MDA-MB-231 breast cancer line with an EGFR/JAK3/PLD2 system that maximizes cancer cell invasion.* J Mol Biol, 2013. **425**(4): p. 755-66.
125. Uhlen, M., et al., *Towards a knowledge-based Human Protein Atlas.* Nat Biotechnol, 2010. **28**(12): p. 1248-50.
126. Caiazza, F., B.J. Harvey, and W. Thomas, *Cytosolic phospholipase A2 activation correlates with HER2 overexpression and mediates estrogen-dependent breast cancer cell growth.* Mol Endocrinol, 2010. **24**(5): p. 953-68.

127. Fullerton, M.D., et al., *Impaired trafficking of choline transporter-like protein-1 at plasma membrane and inhibition of choline transport in THP-1 monocyte-derived macrophages.* Am J Physiol Cell Physiol, 2006. **290**(4): p. C1230-8.
128. Bhujwalla, Z.M., et al., *Nm23-transfected MDA-MB-435 human breast carcinoma cells form tumors with altered phospholipid metabolism and pH: a 31P nuclear magnetic resonance study in vivo and in vitro.* Magn Reson Med, 1999. **41**(5): p. 897-903.
129. Aboagye, E.O. and Z.M. Bhujwalla, *Malignant transformation alters membrane choline phospholipid metabolism of human mammary epithelial cells.* Cancer Res, 1999. **59**(1): p. 80-4.
130. Glunde, K., C. Jie, and Z.M. Bhujwalla, *Molecular causes of the aberrant choline phospholipid metabolism in breast cancer.* Cancer Res, 2004. **64**(12): p. 4270-6.
131. Vance, J.E. and D.E. Vance, *Phospholipid biosynthesis in mammalian cells.* Biochem Cell Biol, 2004. **82**(1): p. 113-28.
132. Speyer, C.L., et al., *Metabotropic glutamate receptor-1: a potential therapeutic target for the treatment of breast cancer.* Breast Cancer Res Treat, 2012. **132**(2): p. 565-73.
133. Takano, T., et al., *Glutamate release promotes growth of malignant gliomas.* Nat Med, 2001. **7**(9): p. 1010-5.
134. Moestue, S.A., et al., *Metabolic biomarkers for response to PI3K inhibition in basal-like breast cancer.* Breast Cancer Res, 2013. **15**(1): p. R16.
135. Griffiths, J.R., et al., *Why are cancers acidic? A carrier-mediated diffusion model for H+ transport in the interstitial fluid.* Novartis Found Symp, 2001. **240**: p. 46-62; discussion 62-7, 152-3.
136. Breukels, V., et al., *Direct dynamic measurement of intracellular and extracellular lactate in small-volume cell suspensions with (13)C hyperpolarised NMR.* NMR Biomed, 2015. **28**(8): p. 1040-8.

APPENDIX

Table of counted PHH3 mitotic cells:

Cell type	Slide number	Magnification	Hot spots number	Cells quantity	Hot spots
PHH3 HMT-2342 1:1500	1	X40	10	51	8,7,3,5,3,4,5,5,4,7
PHH3 HMT-2342 1:1500	2	X40	10	52	4,5,8,3,5,5,4,4,9,5
PHH3 HMT-2342 1:1500	4	X40	10	64	4,4,10,9,5,10,7,6,4,5
PHH3 HMT-2342 1:1500	6	X40	10	65	7,8,8,4,7,6,8,5,6,6
PHH3 HMT-2342 1:1500	8	X40	10	76	8,9,7,8,7,8,9,5,9,6
PHH3 HMT-2342 1:1500	9	X40	10	80	8,12,7,9,8,7,9,5,9,6
PHH3 HMT-2342 1:1500	10	X40	10	48	4,4,6,5,8,4,3,5,3,6
PHH3 HMT-2342 1:1500	12	X40	10	50	4,5,6,7,5,5,4,3,4,7
PHH3 HMT-2342 1:1500 CMIC 2014	13	X40	10	61	6,5,5,7,7,6,9,6,5,5
PHH3 HMT-2342 1:1500	15	X40	10	48	5,3,8,6,5,4,6,2,4,5
PHH3 HMT-2342 1:1500 CMIC 2014	17	X40	10	61	8,5,5,7,10,5,6,6,3,6
PHH3 HMT-2342 1:1500 CMIC 2014	18	X40	10	55	6,6,4,7,8,3,5,6,4,6

PHH3 HMT-2342 1:1500 CMIC 2014	19	X40	10	50	3,4,5,8,4,5,7,4,6,4
PHH3 HMT-2342 1:1500 CMIC 2014	21	X40	10	54	4,6,6,8,7,2,4,8,3,6
PHH3 HMT-2342 1:1500 CMIC 2014	23	X40	10	76	8,8,6,10,7,5,12,6,9,5
PHH3 HMT-2342 1:1500 CMIC 2014	25	X40	10	72	7,8,11,7,5,6,8,9,5,6
PHH3 HMT-2342 1:1500 CMIC 2014	27	X40	10	63	4,12,6,9,6,5,5,5,6,5
PHH3 HMT-2342 1:1500 CMIC 2014	28	X40	10	61	5,7,6,10,5,5,4,6,7,6
PHH3 HMT-2342 1:1500 CMIC 2014	30	X40	10	82	8,8,4,10,6,13,6,14,6,7
PHH3 HMT-2342 1:1500 CMIC 2014	31	X40	10	51	5,5,5,6,4,7,4,3,7,5
PHH3 HMT-2342 1:1500 CMIC 2014	32	X40	10	52	6,9,5,6,8,6,4,3,2,3
PHH3 HMT-2342 1:1500 CMIC 2014	34	X40	10	56	7,7,4,3,5,6,5,7,8,4
PHH3 HMT-2342 1:1500 CMIC 2014	36	X40	10	57	4,5,5,8,6,6,5,7,6,5
PHH3 HMT-2342 1:1500 CMIC 2014	37	X40	10	61	4,10,5,4,9,7,6,5,6,5

PHH3 HMT-2342 1:1500 CMIC 2014	39	X40	10	60	6,8,8,5,5,9,7,5,4,3

Cell counting for Growth Curve of MDA-MB-231 cell line

Days	Slide	square1	square2	square3	average of slides	SD Slide	average of day	SD Day	Cells in 2ml
day1	Flask1 slide1	22	18	15	18,3	3,5	18,3	4,5	366000
	Flask1 slide2	11	15	20	15,3	4,5			
	Flask2 slide1	21	21	17	19,7	2,3			
	Flask2 slide2	28	16	15	19,7	7,2			
day2	Flask1 slide1	50	31	32	37,7	10,7	39,5	9,7	790000
	Flask1 slide2	48	40	40	42,7	4,6			
	Flask2 slide1	34	21	50	35,0	14,5			
	Flask2 slide2	46	31	51	42,7	10,4			
day3	Flask1 slide1	85	74	79	79,3	5,5	78,8	9,2	1576000
	Flask1 slide2	63	64	91	72,7	15,9			
	Flask2 slide1	84	81	92	85,7	5,7			
	Flask2 slide2	83	74	76	77,7	4,7			
day4	Flask1 slide1	102	99	101	100,7	1,5	113,3	15,2	2266000
	Flask1 slide2	114	104	107	108,3	5,1			
	Flask2 slide1	141	128	137	135,3	6,7			
	Flask2 slide2	103	100	124	109,0	13,1			
day5	Flask1 slide1	132	131	144	135,7	7,2	136,6	17,6	2732000
	Flask1 slide2	130	122	136	129,3	7,0			
	Flask2 slide1	130	122	136	129,3	7,0			
	Flask2 slide2	172	169	115	152,0	32,1			
day6	Flask1 slide1	186	188	197	190,3	5,9	210,1	34,3	4202000
	Flask1 slide2	196	243	257	232,0	32,0			
	Flask2 slide1	156	169	209	178,0	27,6			
	Flask2 slide2	218	241	261	240,0	21,5			